Cosmic Ray Conundra

INTERSTELLAR E-DENSITIES

$0.44\ \mathrm{eV/cm^3}$

★ - γ

$0.23\ \mathrm{eV/cm^3}$

MWBR

$\sim 1\ \mathrm{eV/cm^3}$

$\vec{B}^2/2$

$\rho_{CR} \sim 1\ \mathrm{eV/cm^3}$

COSMIC RAYS

mainly p , $\bar{E}_p \sim 1\ \mathrm{GeV}$

$$F_{CR} = \frac{v}{4\pi}\rho_{CR}$$

$$F_{CR}^{TOT} \sim \frac{1}{\mathrm{cm^2\,s}}$$

$E^{2.75} * d\phi/dE$

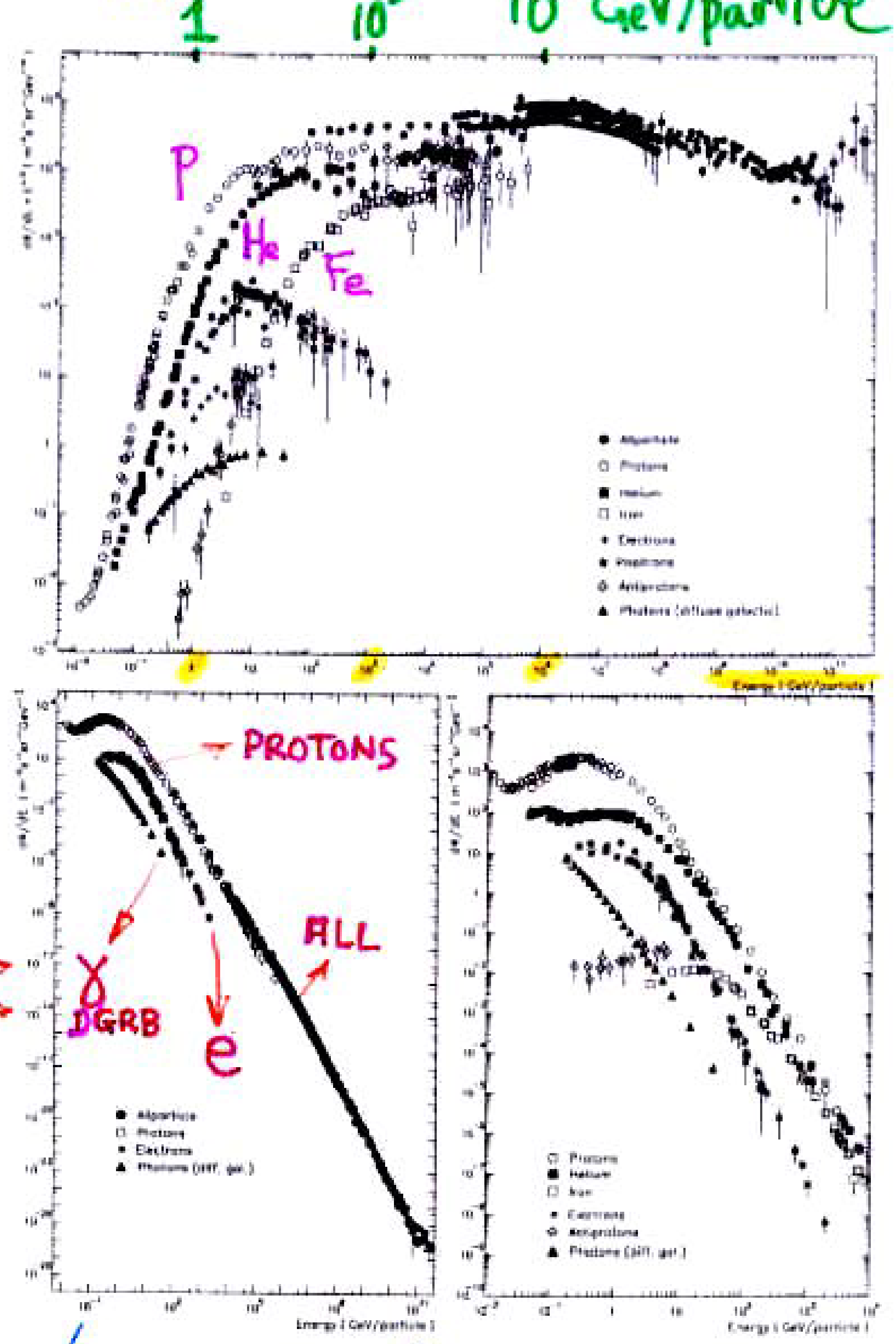

$\frac{d\phi}{dE}$

Figure 2. Overview of the population of cosmic rays observed on Earth as measured by direct and ground-based experiments. The all particle spectrum combined with spectra of protons, helium, iron, electrons, positrons, antiprotons, and photons are shown, where in the upper graph all spectra are multiplied with $E^{2.75}$ to emphasize features in the spectra.

100 MeV

10^{11} GeV

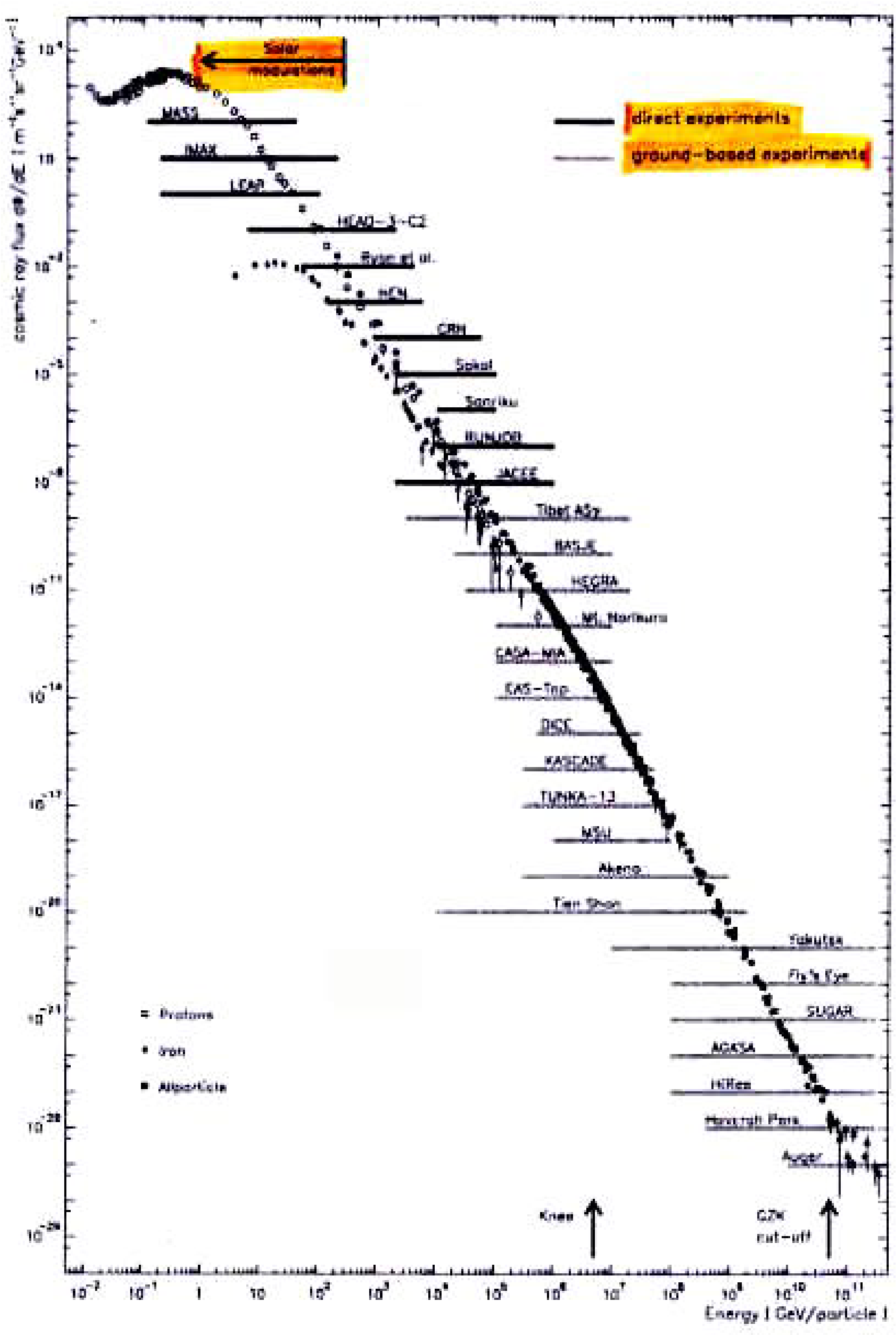

Figure 1: The energy ranges of several direct and indirect experiments, which provided data on the cosmic ray spectrum or will provide data in the near future.

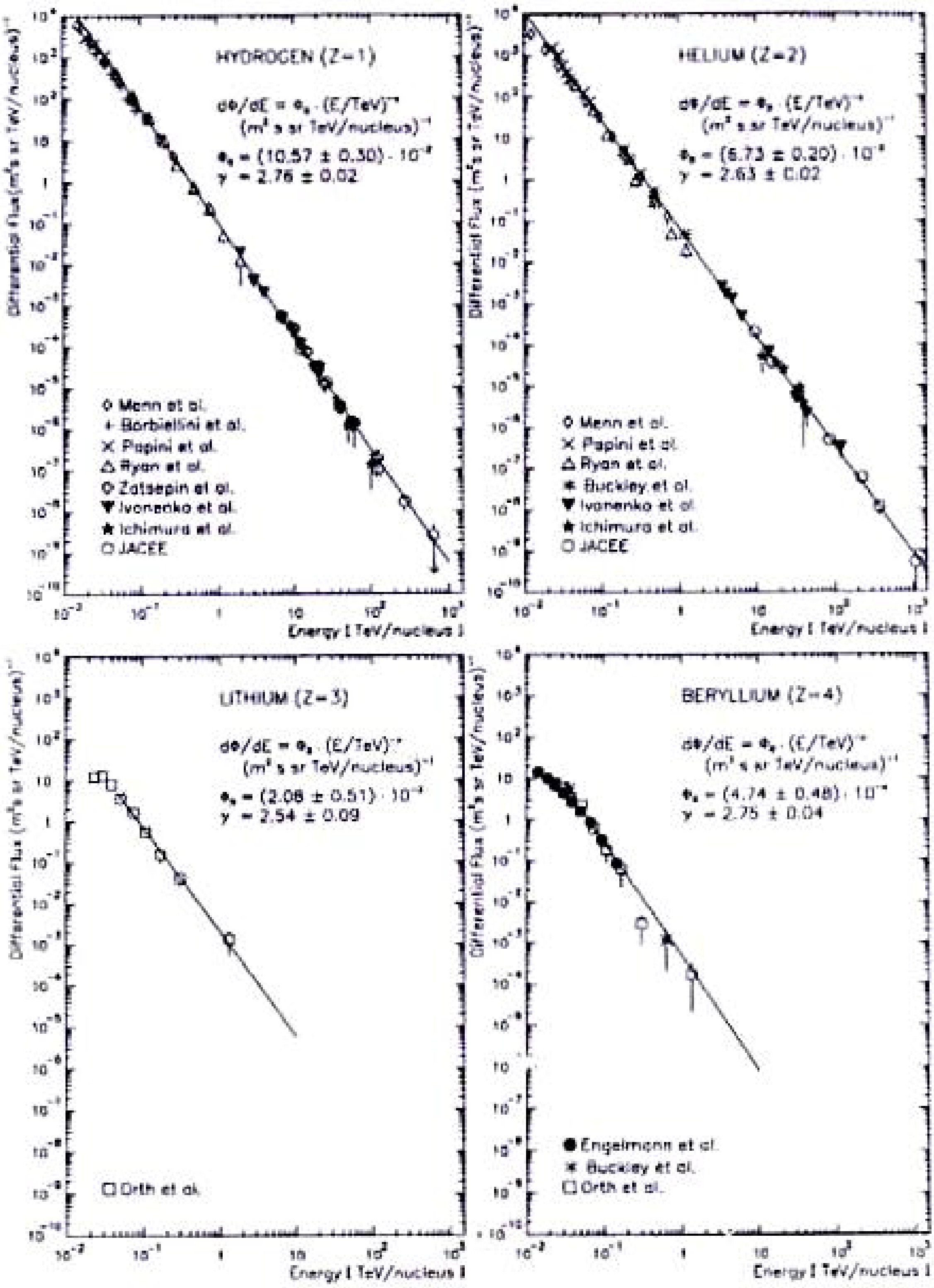

Figure 3: Differential energy spectra of the elements H, He, Li and Be.

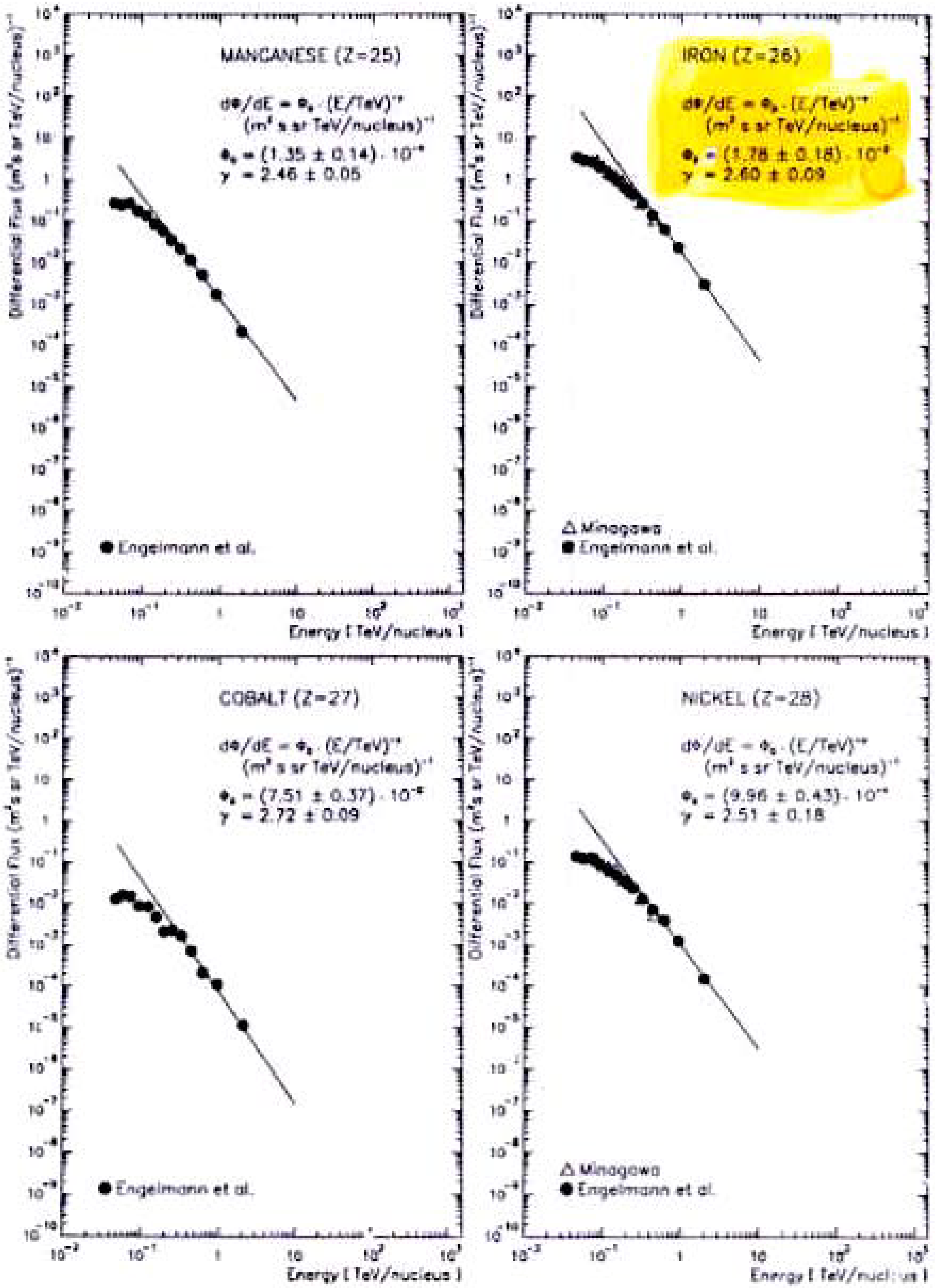

Figure 9: Differential energy spectra of the elements Mn, Fe, Co and Ni.

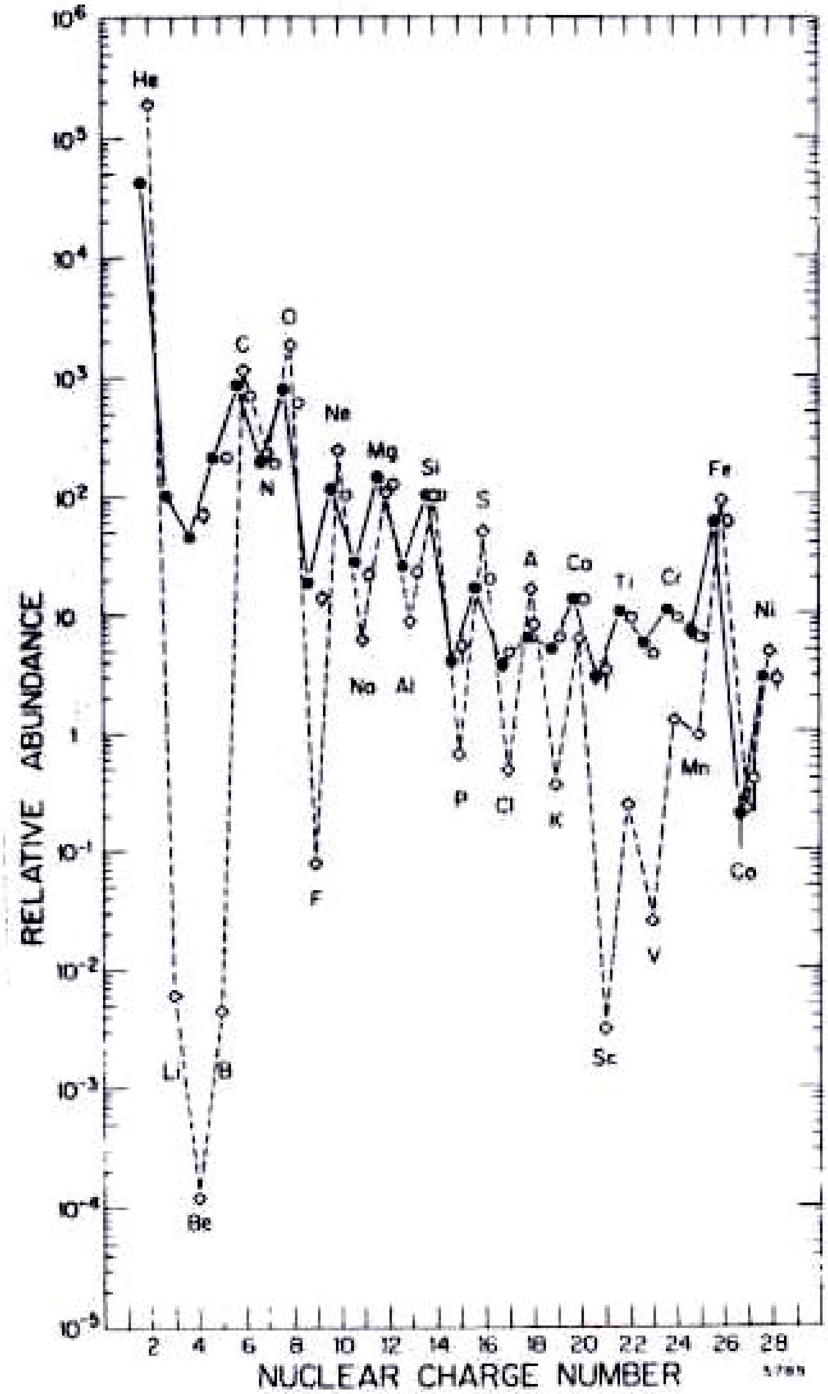

FIG. 1. Relative abundance distribution of the elements in the cosmic radiation (normalized to Si = 100) from He through Ni (●, 70–280 MeV per nucleon; ○, 1000–2000 MeV per nucleon; ◇, ---, Solar System abundance distribution). [Reproduced, with permission, from Simpson, J. A. (1983). *Annu. Rev. Nucl. Part. Sci.* **33**; © 1983 by Annual Reviews Inc.]

$$\tau(\langle E \rangle) \sim 10^7 y \quad \text{IN THE DISC} \qquad \tau(E) \propto \frac{1}{E^{\sim 0.6}}$$

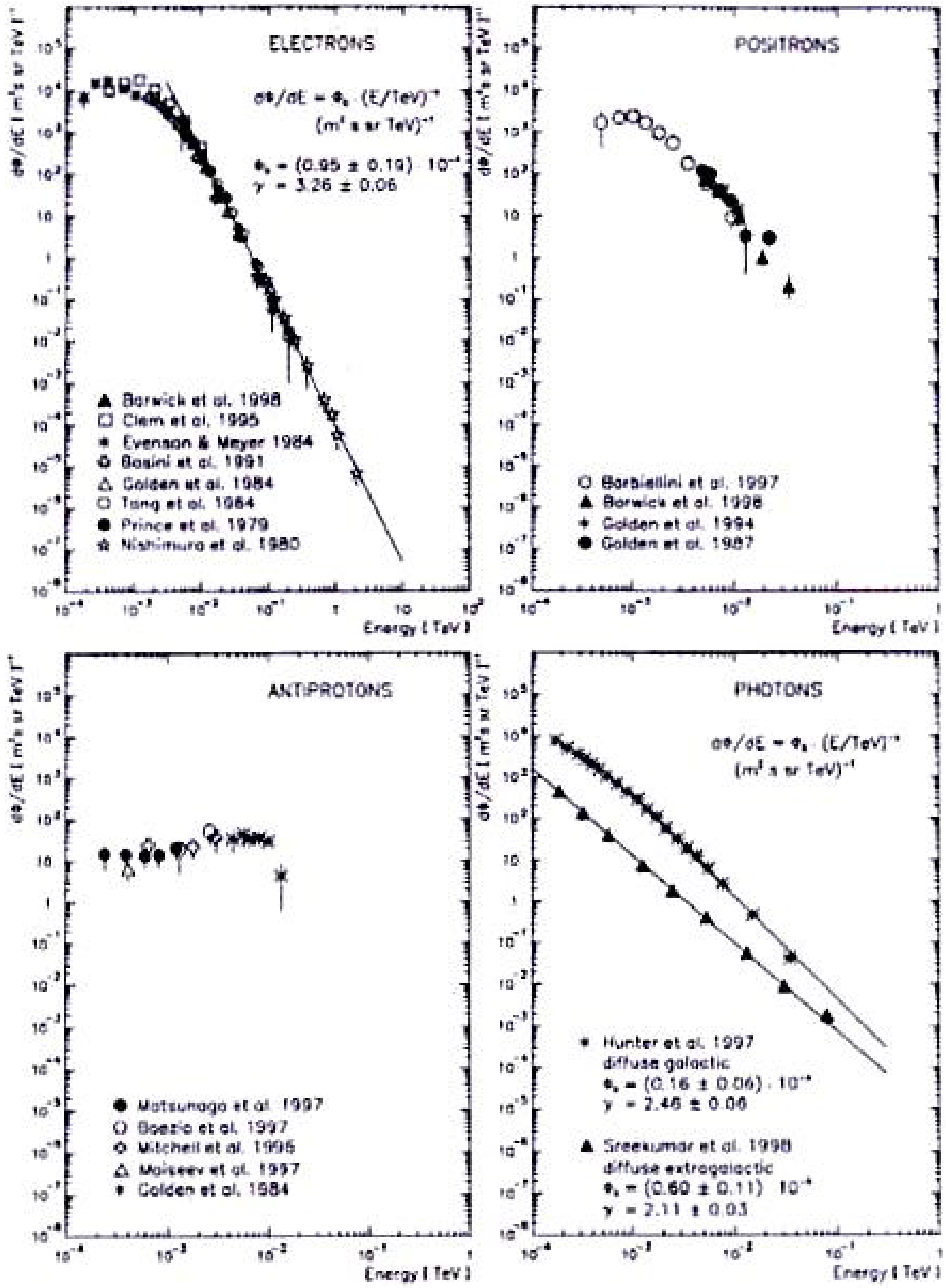

Figure 12: Differential energy spectra of electrons, positrons, antiprotons and photons.

$e^+, \bar{p}$ SECONDARY ✓

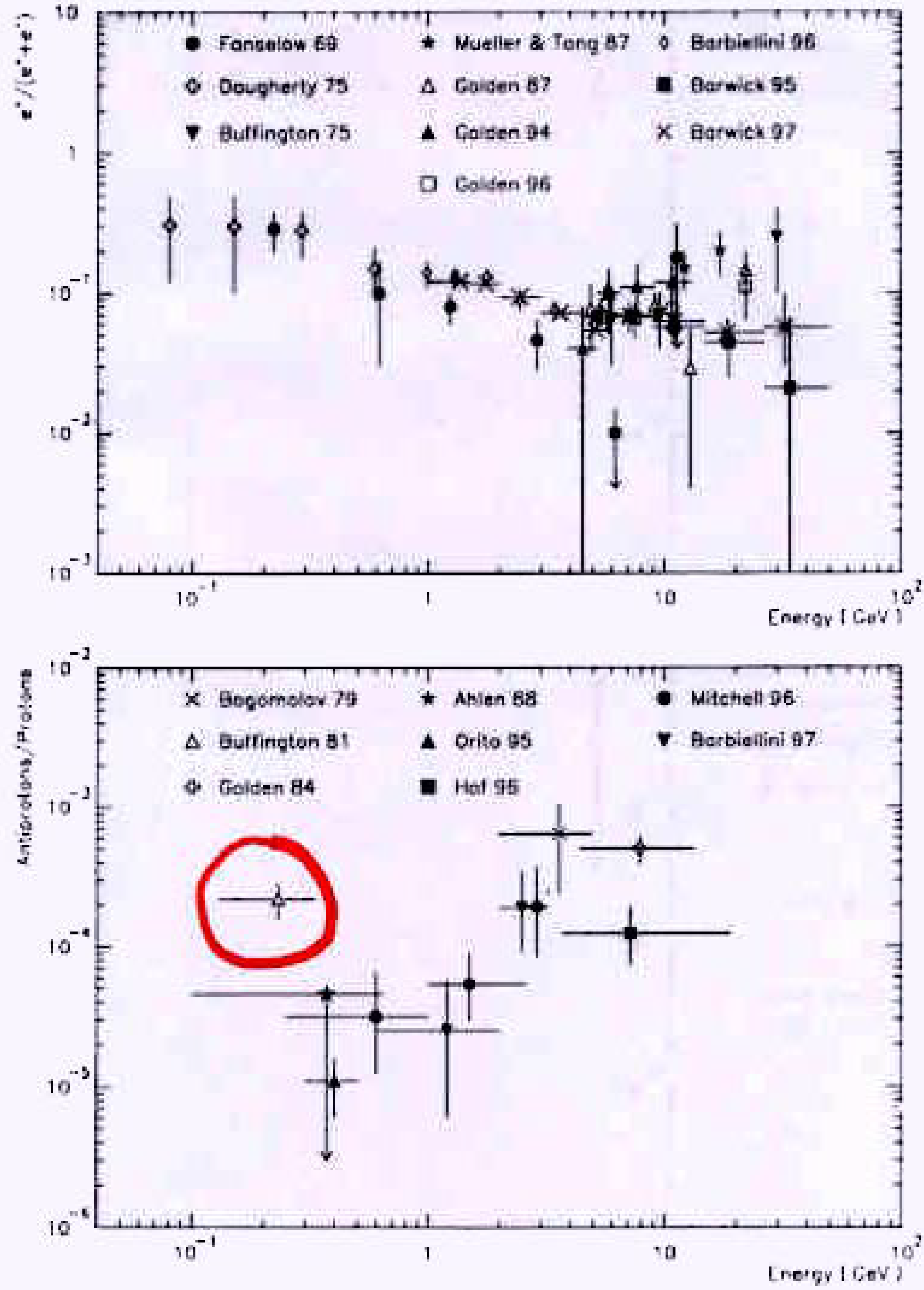

Figure 13: The amount of positrons and antiprotons in the cosmic radiation, shown as the measured ratio of $e^+/(e^+ + e^-)$ and $\bar{p}/p$. Here only those experiments are shown, which measured the ratios directly.

COUTO et al ASTRO PH/9902162

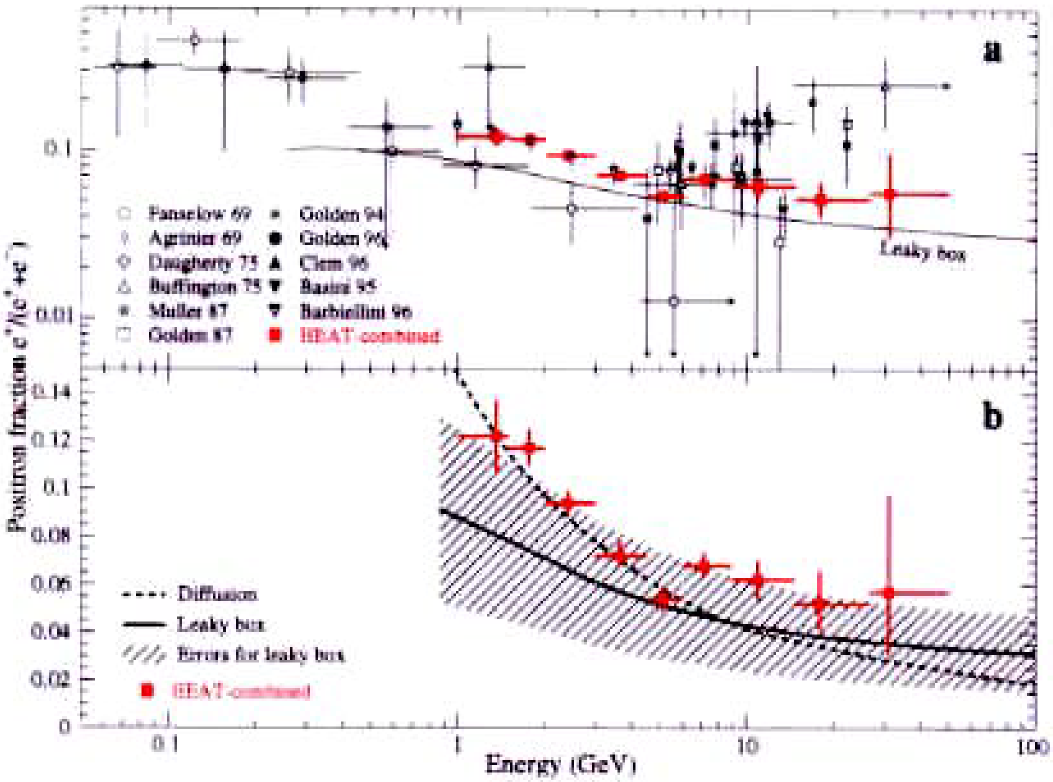

Fig. 1.— **a** Compilation of measurements [1, 2, 4 -13] of the positron fraction between 0.05 and 50 GeV. The solid curve is a model calculation [3] assuming that all positrons are from secondary sources, and propagate according to a simple Galactic leaky-box model. "HEAT-combined" refers to the combination [13] of the data sets from the two HEAT flights. **b** The positron fraction measured with the HEAT instrument, shown on a vertical linear scale. The solid curve is a leaky-box secondary model prediction [3], surrounded by an estimated band of uncertainty shown as the cross-hatching. The dashed curve is a secondary model prediction using Galactic diffusion [27].

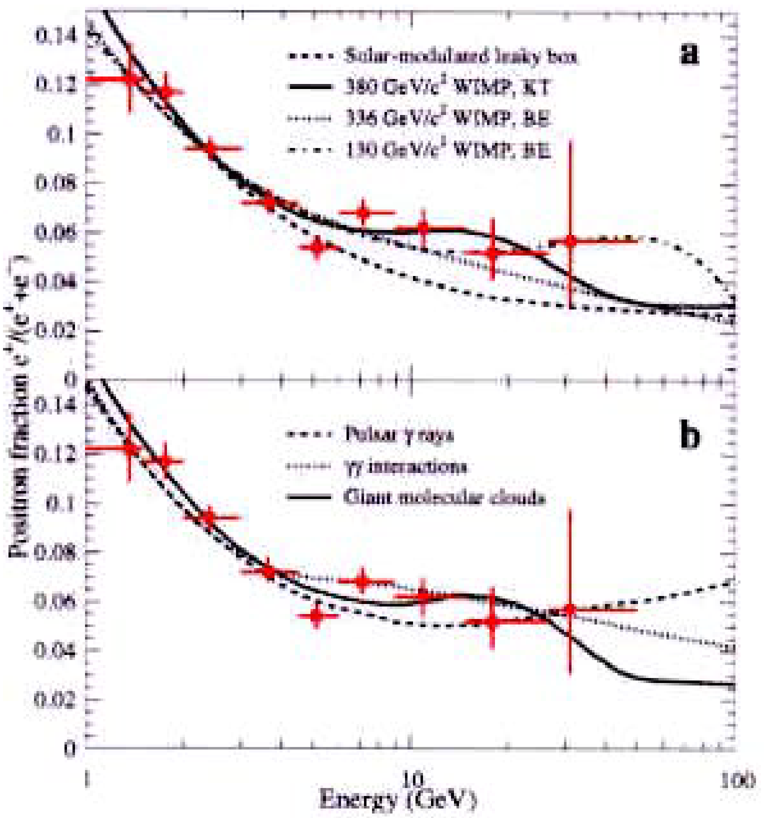

Fig. 2.— **a** The HEAT positron fraction compared with best-fit model predictions with an additional positron component arising from annihilating dark matter neutralinos. The dashed curve is the baseline solar-modulated leaky-box secondary-production prediction [10], renormalized by a factor of 0.85. The solid curve shows an increased positron content due to annihilating 380 GeV/c^2 neutralinos in the model of Kamionkowski and Turner [20]. The dotted and dot-dash curves show an increased positron content due to annihilating 336 or 130 GeV/c^2 neutralinos, respectively, in the model of Baltz and Edsjö [30]. **b** The HEAT positron fraction compared with best-fit model predictions from astrophysical sources of positrons that are in addition to secondary production mechanisms. The dashed curve is the positron enhancement resulting from high-energy γ rays converting to e^+e^- pairs near the magnetic poles of pulsars [19]. The dotted curve represents a positron enhancement due to high-energy γ rays interacting with low-energy optical or UV photon fields [16]. The solid curve shows the enhancement from cosmic-ray interactions within giant molecular clouds [18].

CONSENSUS ON ORIGIN [OR LACK THEREOF]

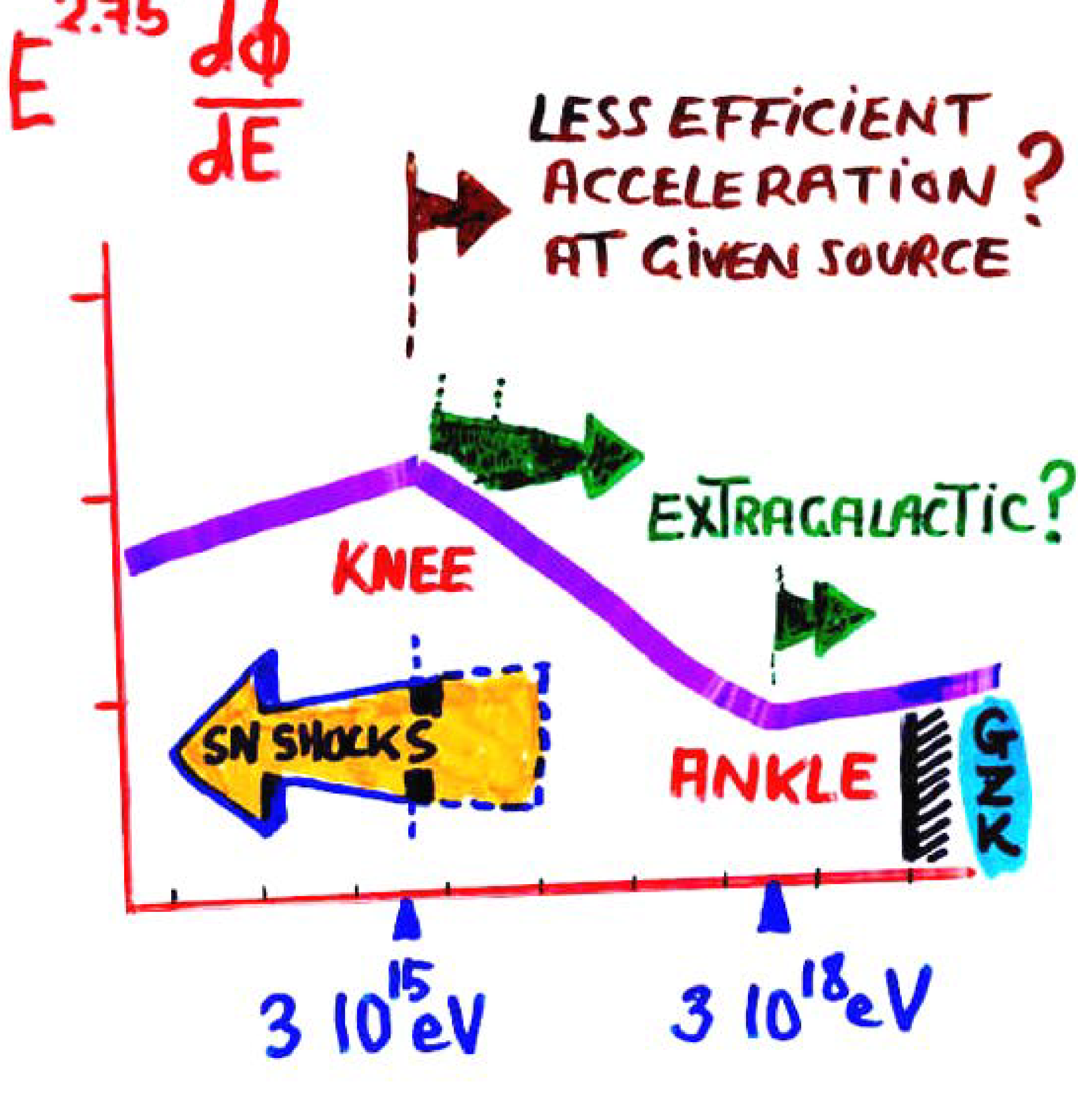

$E^{2.75} d\phi / dE$

GZK

10^{20} eV

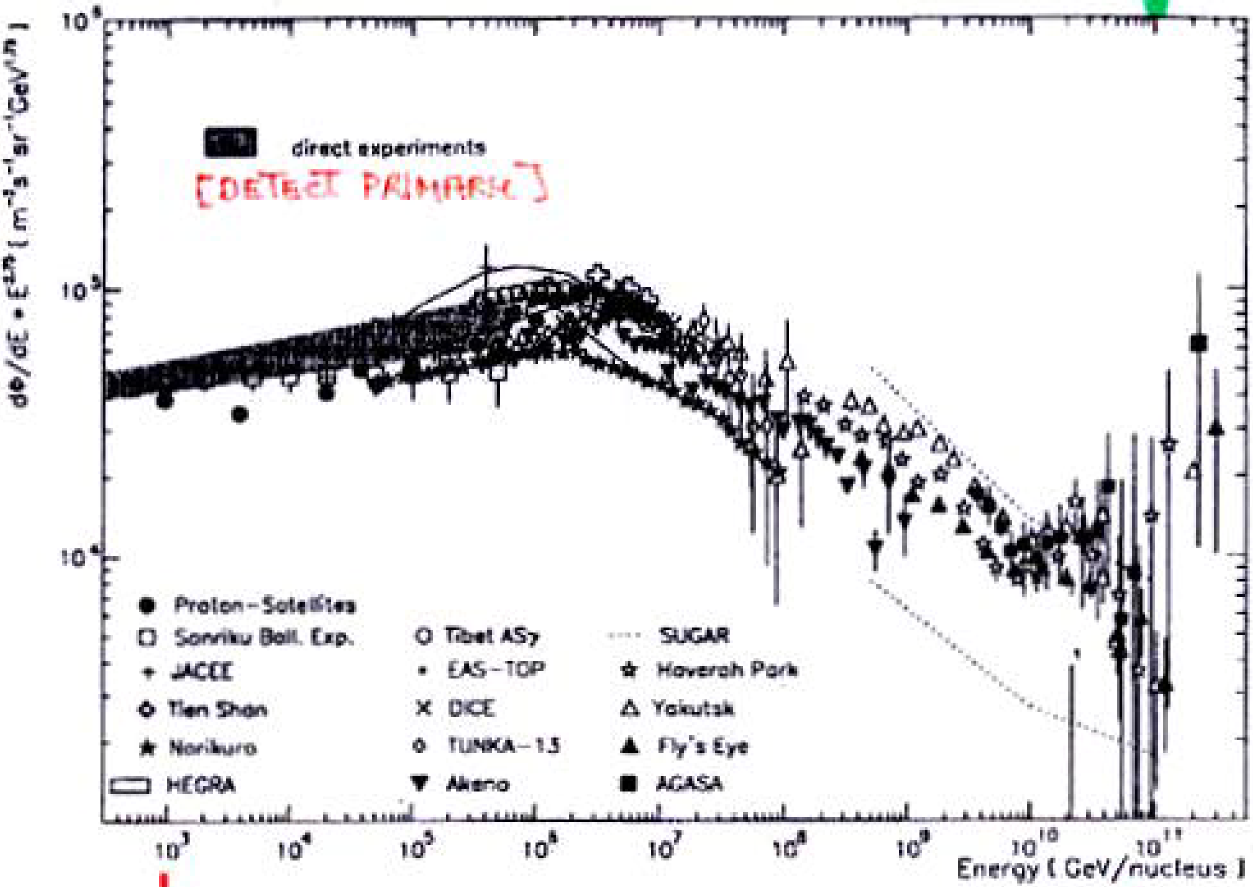

Figure 15: The allparticle energy spectrum as measured by different ground-based experiments and three direct ones. For comparison the allparticle flux obtained by adding up the single spectra of individual nuclei as measured by the bulk of direct experiments is also given. To emphasize changes in the spectral slope, the differential flux is multiplied by $E^{2.75}$. (References see Tab. 1 and 2).

1 TeV

10^{11} GeV

= 100 EeV

$* 10^{8}$

E_{ACC} vs $B * L$

GZK

10^{20} eV

Hillas-plot (candidate sites for E=100 EeV)

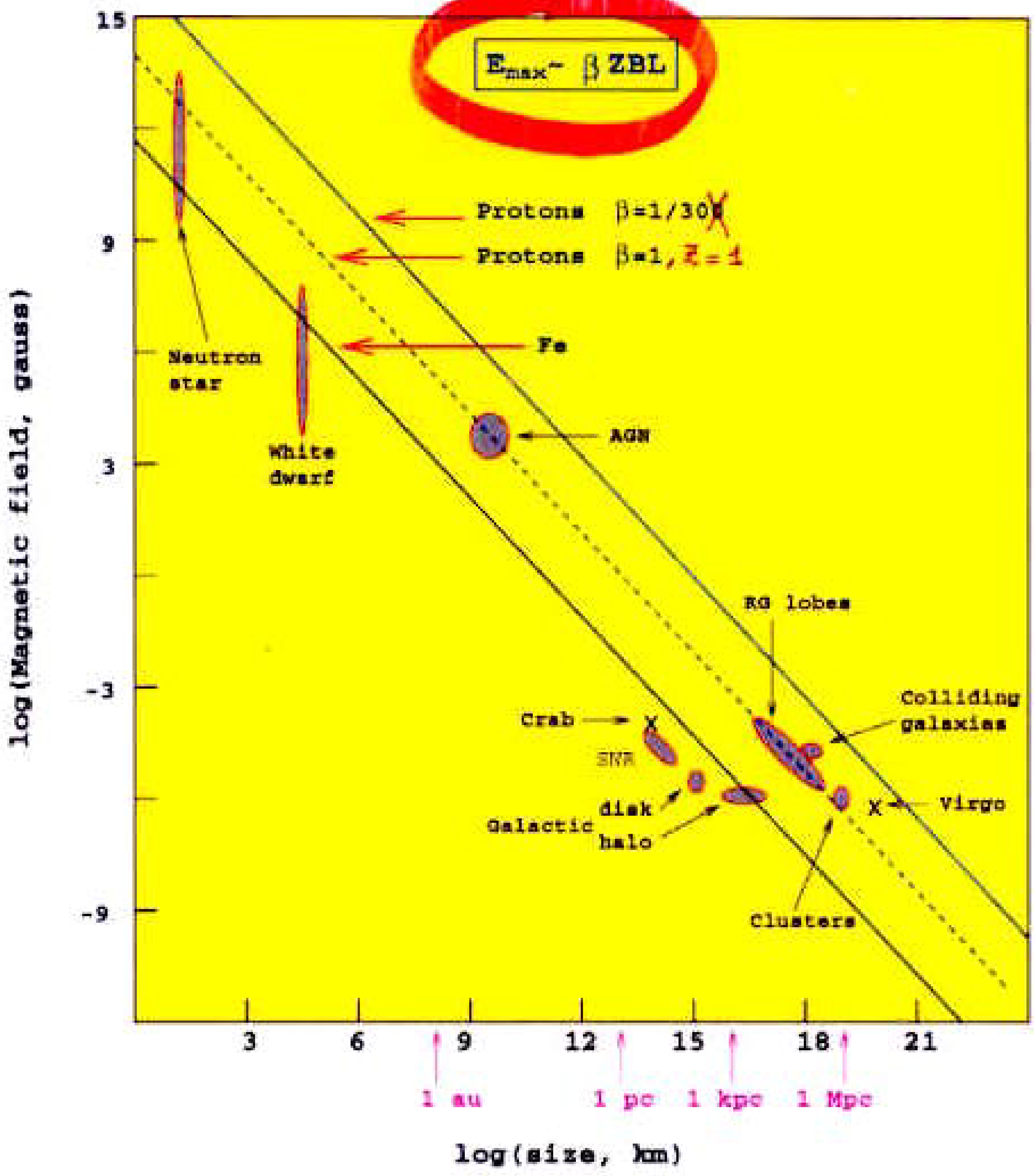

Figure 22: The Hillas diagram. This version courtesy Murat Boratav.

L

GREISEN, ZATSEPIN & KUZMIN. CUTOFF

GZK

$n_0 \sim 411/cm^3 \quad T_0 \sim 2.7\,K$

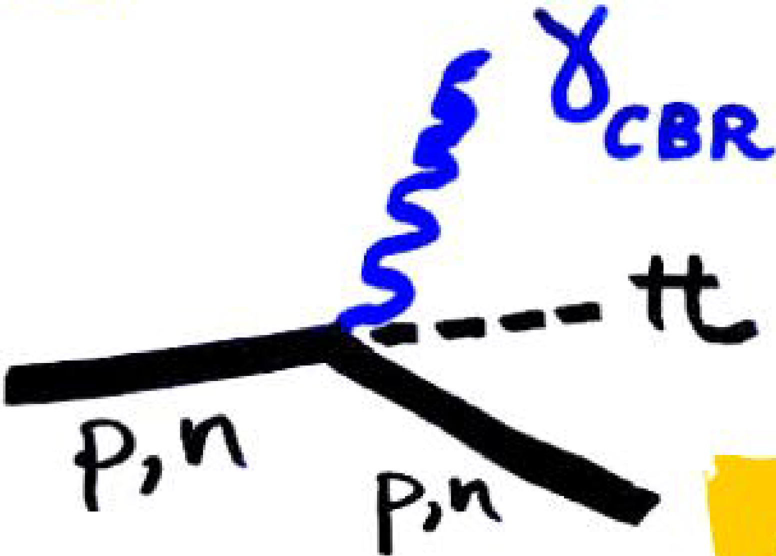

$[T_0 : \text{MWBR}]$

σ $E > E_{TH}$ is LARGE

$\boxed{E_{TH} \sim 10^{20}\,eV}$

$$\mathcal{N} + \gamma_{CBR} \rightarrow \text{PIECES}$$
$$\gamma + \gamma_{CBR} \rightarrow e^+e^-$$

CUT AT LOWER ENERGY THAN $p + \gamma_{CBR}$

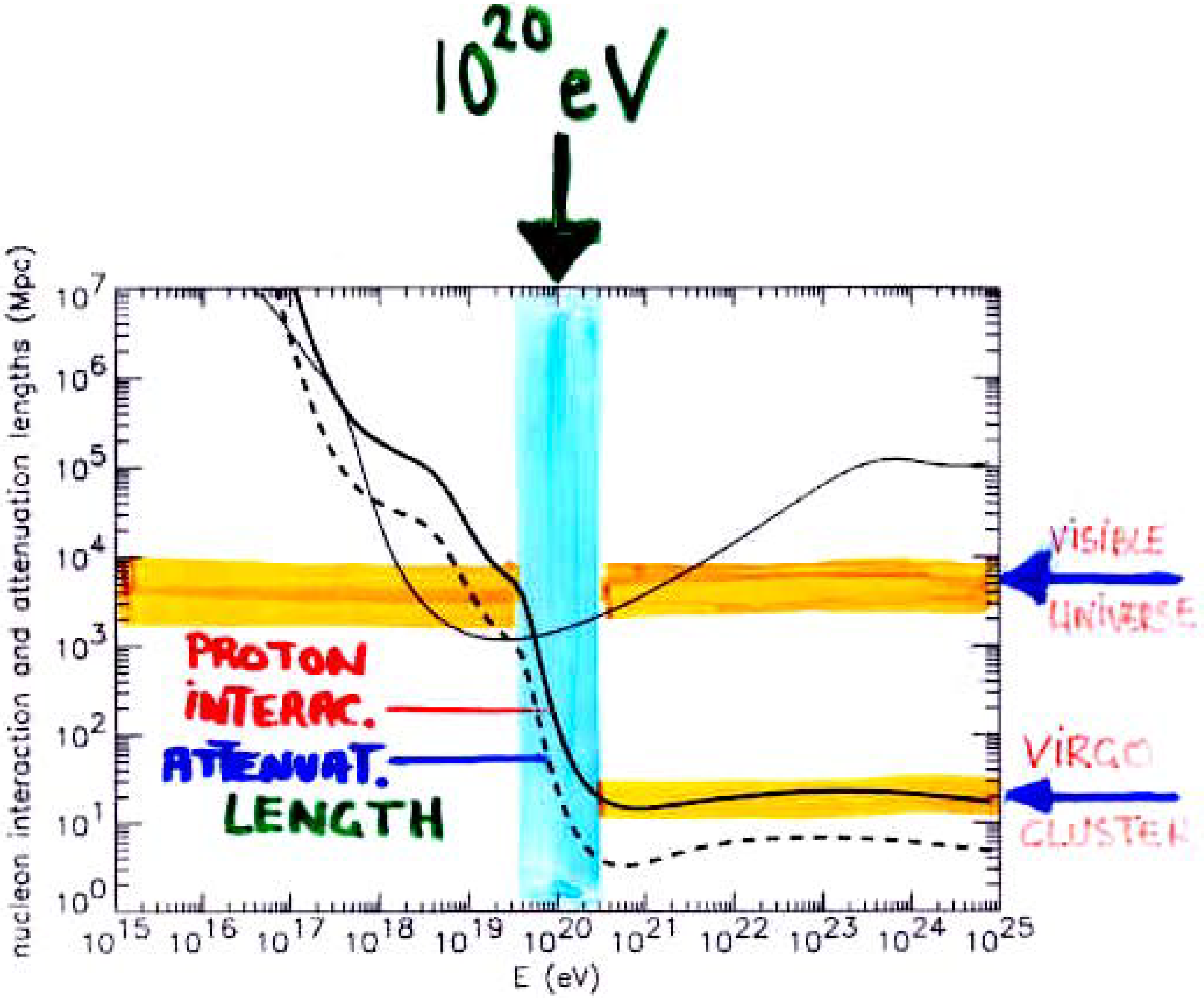

Figure 9: The nucleon interaction length (dashed line) and attenuation length (solid line) for photo-pion production and the proton attenuation length for pair production (thin solid line) in the CMB and the observational estimate of the total extragalactic radio background intensity shown in Fig. 10 below.

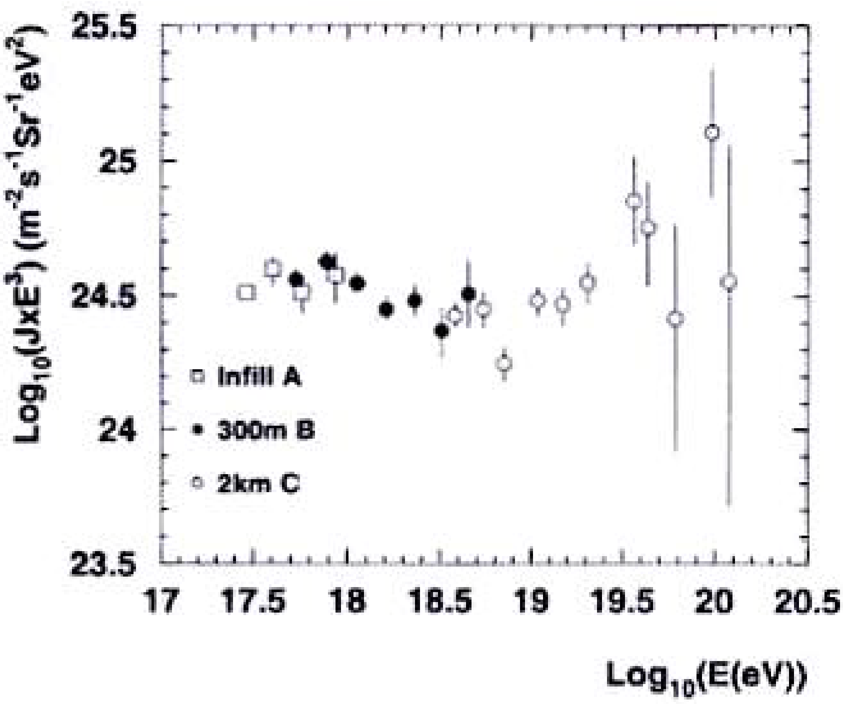

Figure 5: The Haverah Park energy spectrum. (From Yoshida and Dai [27]).

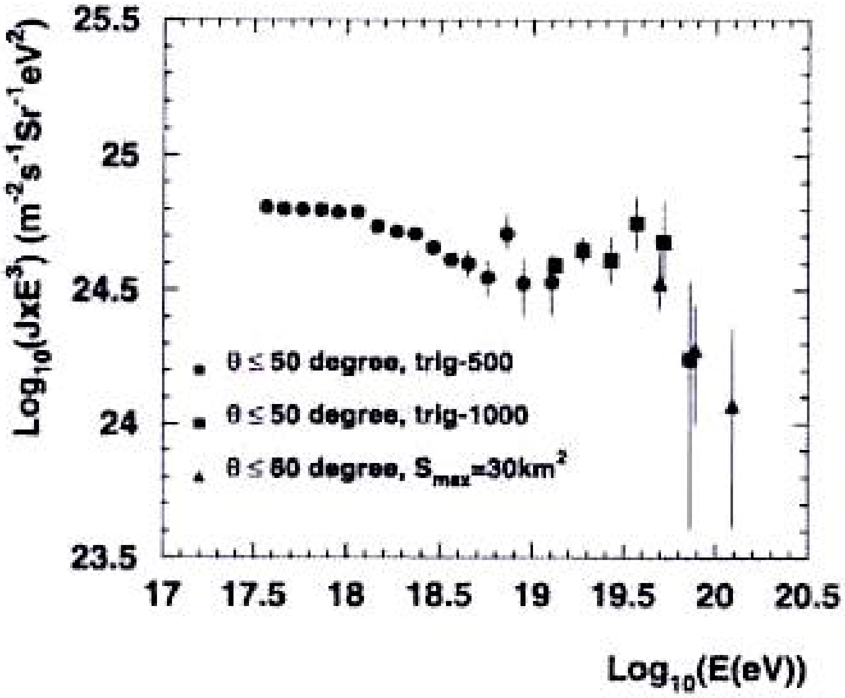

Figure 6: The Yakutsk energy spectrum. (From Yoshida and Dai [27]).

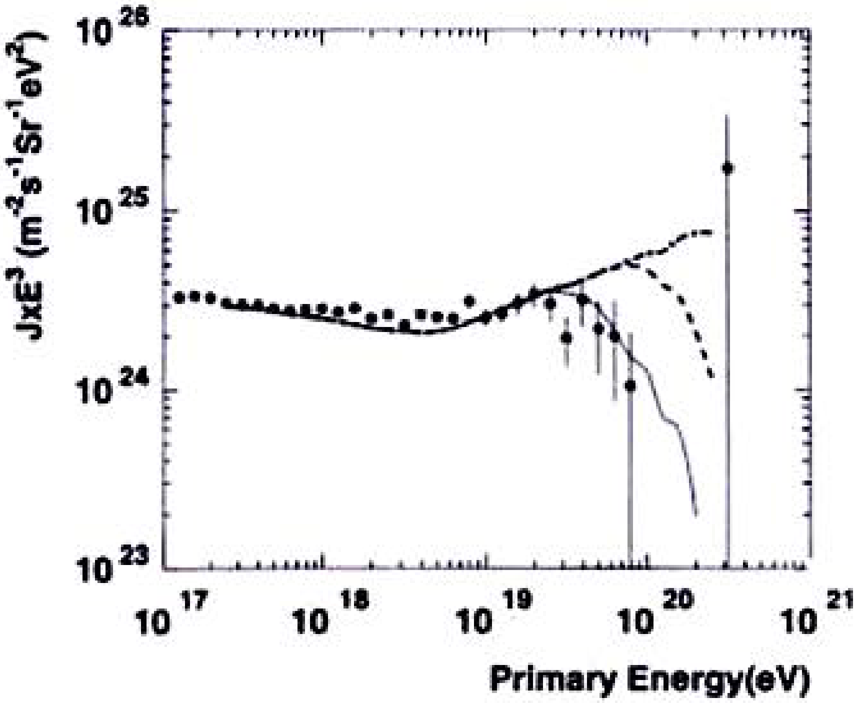

Figure 3: Fly's Eye monocular energy spectrum. Dots: data. Lines: predicted spectra for source energy cutoff at different energies. Solid line: cutoff at $10^{19.6}$ eV. Dashed line: cutoff at 10^{20} eV. Chain line: cutoff at 10^{21} eV. (From Yoshida and Dai [27]).

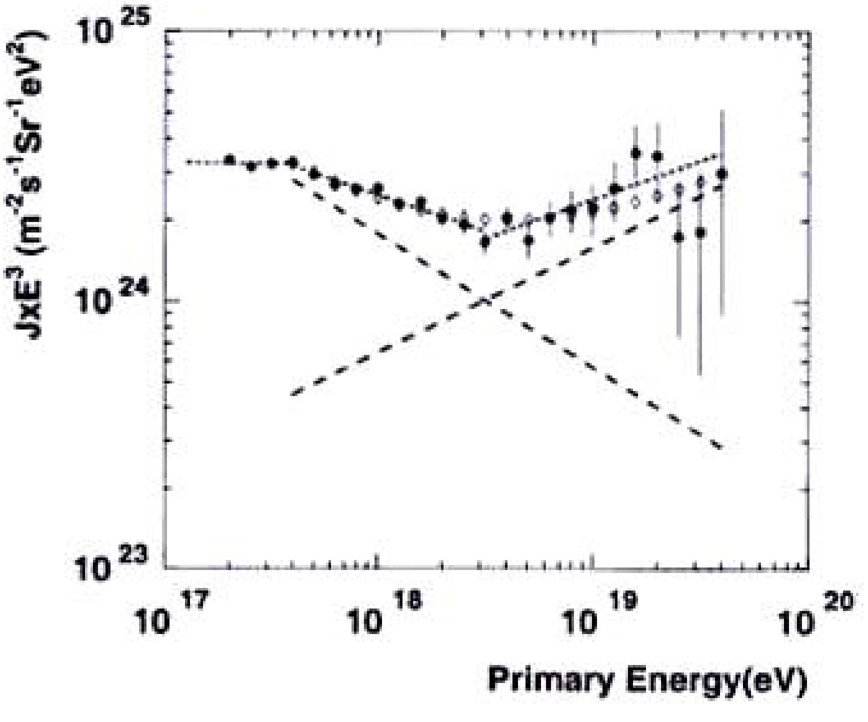

Figure 4: Fly's Eye stereo energy spectrum. Dots: data. Dotted line: best fit in each region. Dashed lines: a two-component fit. (From Yoshida and Dai [27]).

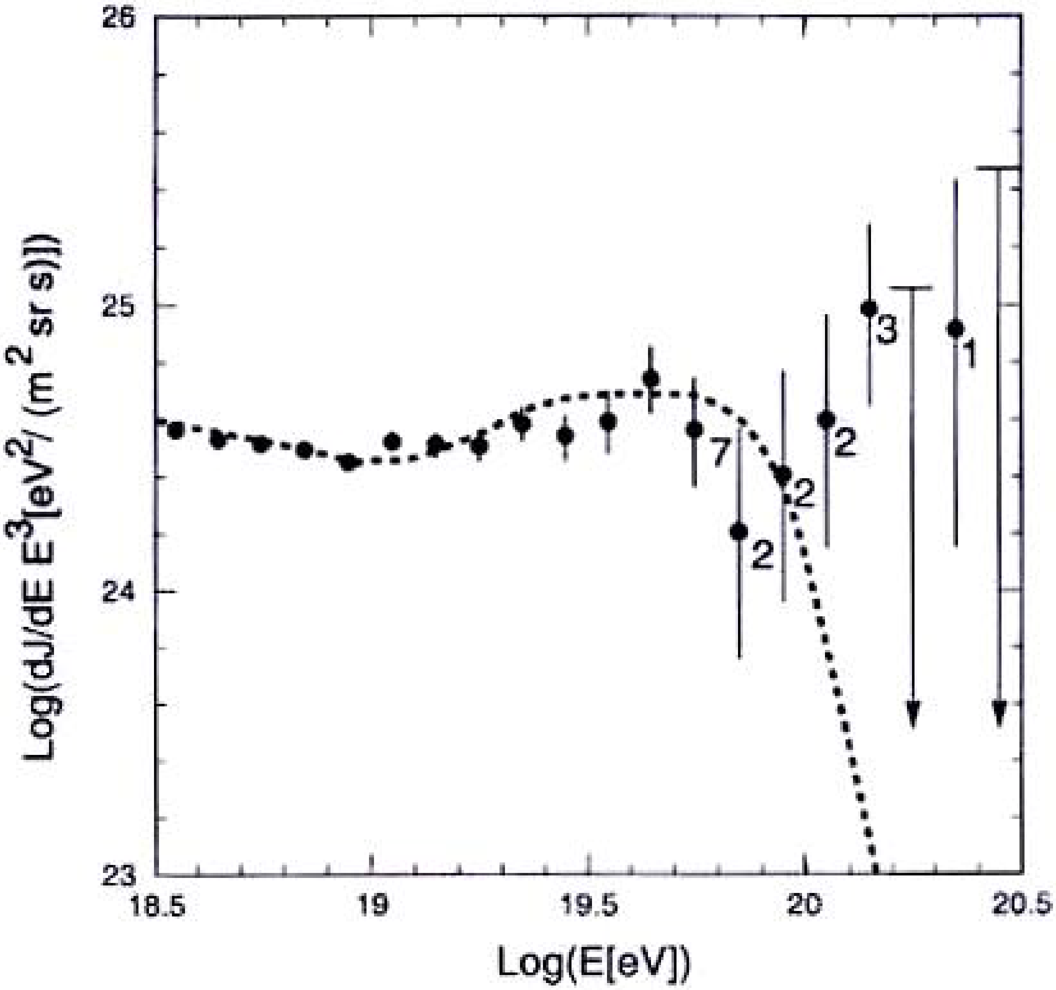

Figure 2: Energy spectrum of UHECR measured by the AGASA experiment. The dashed curve representa the spectrum expected for extragalactic sources distributed uniformly in the Universe.(From M Takeda et al [6].)

$\gamma B_{\otimes}$

CANNOT BE γ

CANNOT BE ν

CAN BE p, N

BUT WHERE FROM?

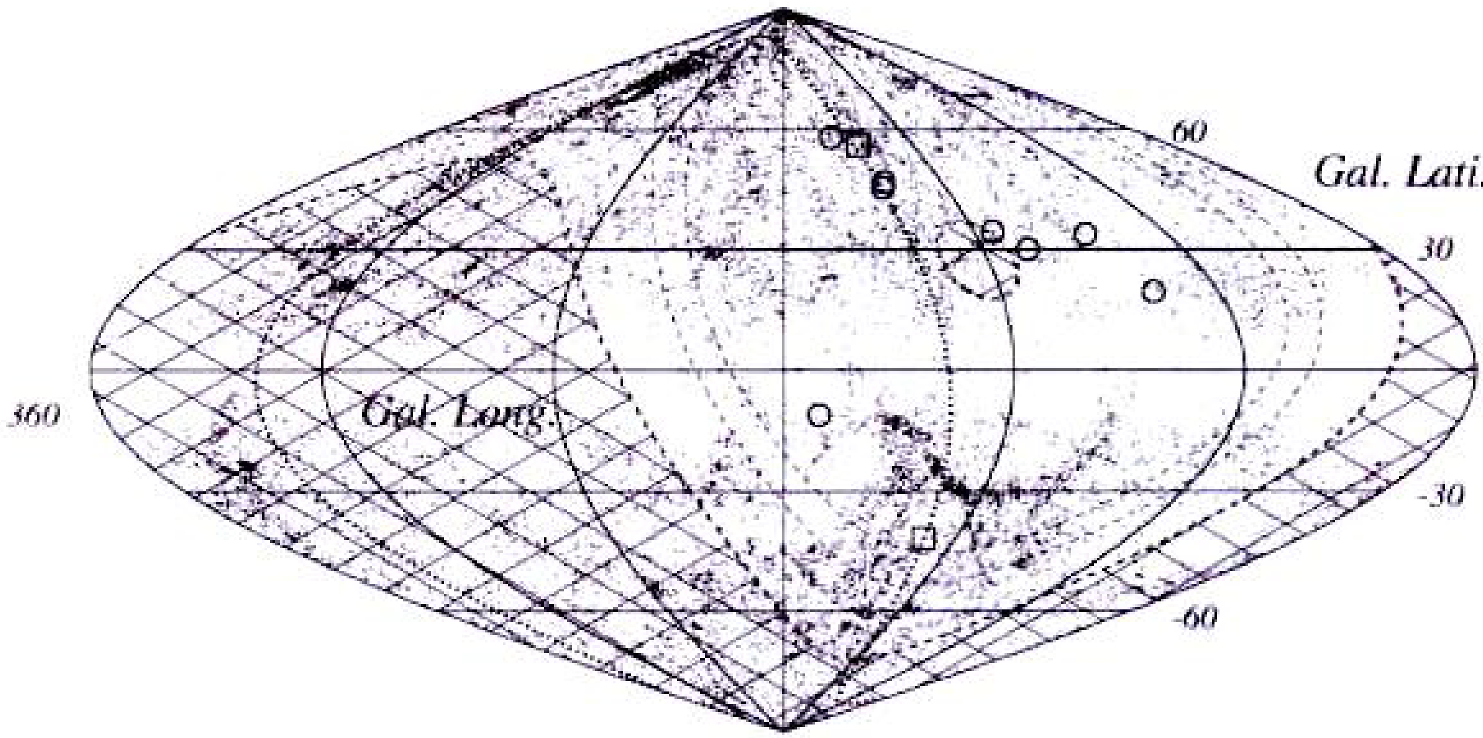
60
Gal. Lati.
30
360
Gal. Long.
-30
-60

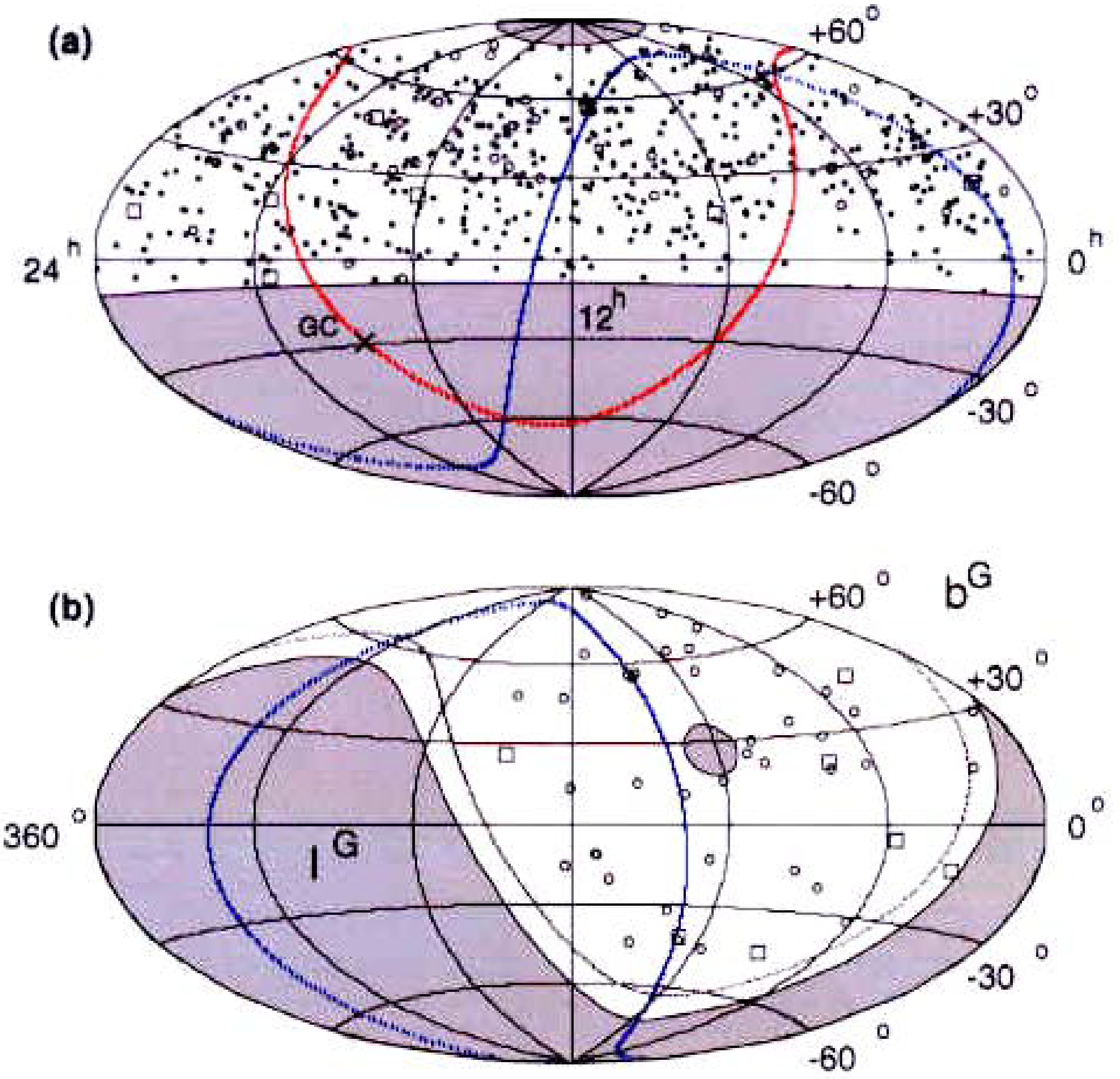

Fig. 2.—

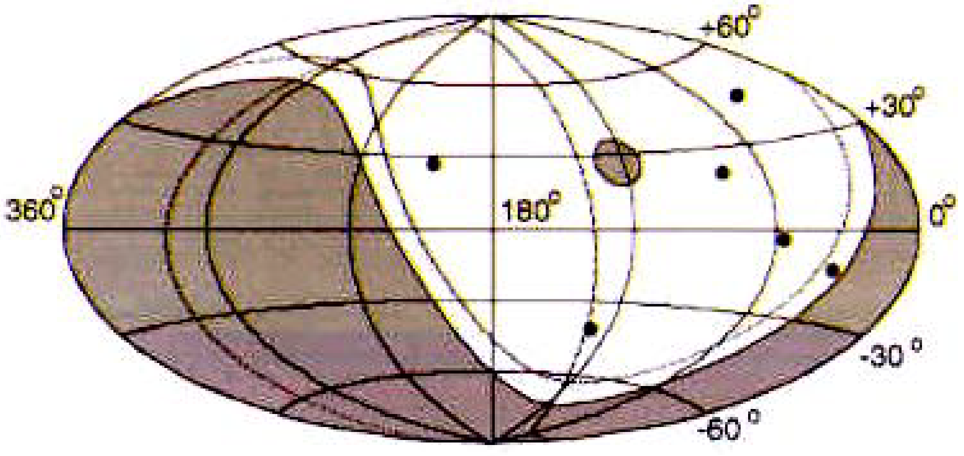

FIG. 3. Arrival directions of six $10^{20}eV$ events on the Galactic coordinates. The shaded regions indicate the non-observable celestial regions due to the zenith angle cut of $\leq 45°$. The equatorial and supergalactic planes are also shown.

· GALAXIES < 100 Mpc

...... SUPERGALACTIC PLANE

□ TRIPLETS } $\Delta\theta < 4^0$

○ DOUBLETS }

UNIFORM DISTRIBUTION

P ~ 10%

UNIFORM ± 10^0 OF SGP

P ~ 1%

UCHIHORI et al. 92 EVENTS ABOVE $4\,10^{19}$ eV

(ALL EXPERIMENTS)

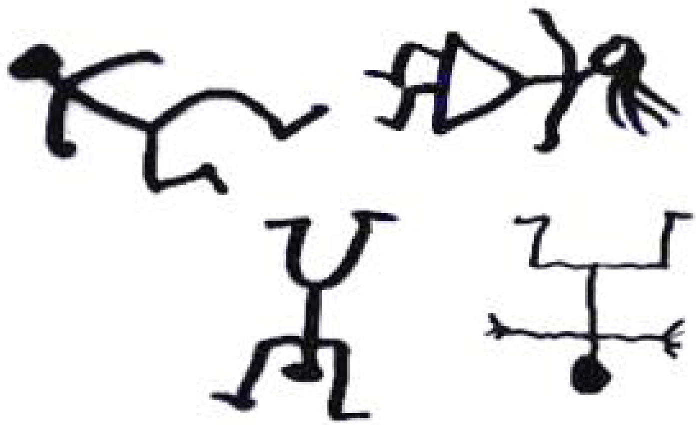

- M_{Pl} RELICS OF BB
- NEUTRAL PARTICLES
  $\supset$ LIGHT GLUINOS
- MONOPOLES
- KNOTS IN PRIMORDIAL STRINGS
- TOPOLOGICAL DEFECTS
- $\nu_{UHE} + \nu_{HALO} \to WW, ZZ \ldots$
- BREKDOWN OF $\mathcal{L}$-INVAR.
-

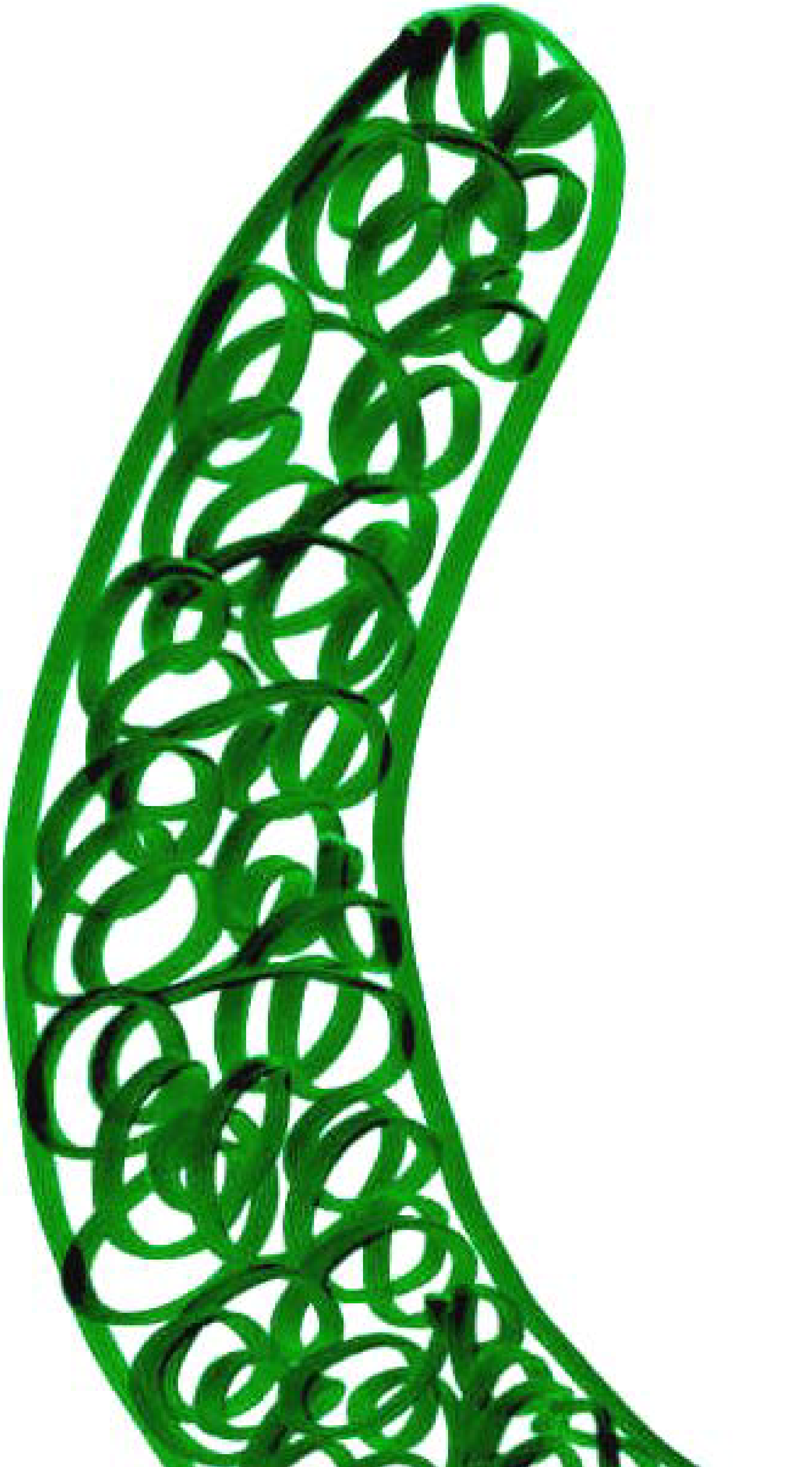

JETS in ASTROPHYSICS
&
GAMMA-
RAY
BURTS

3C175

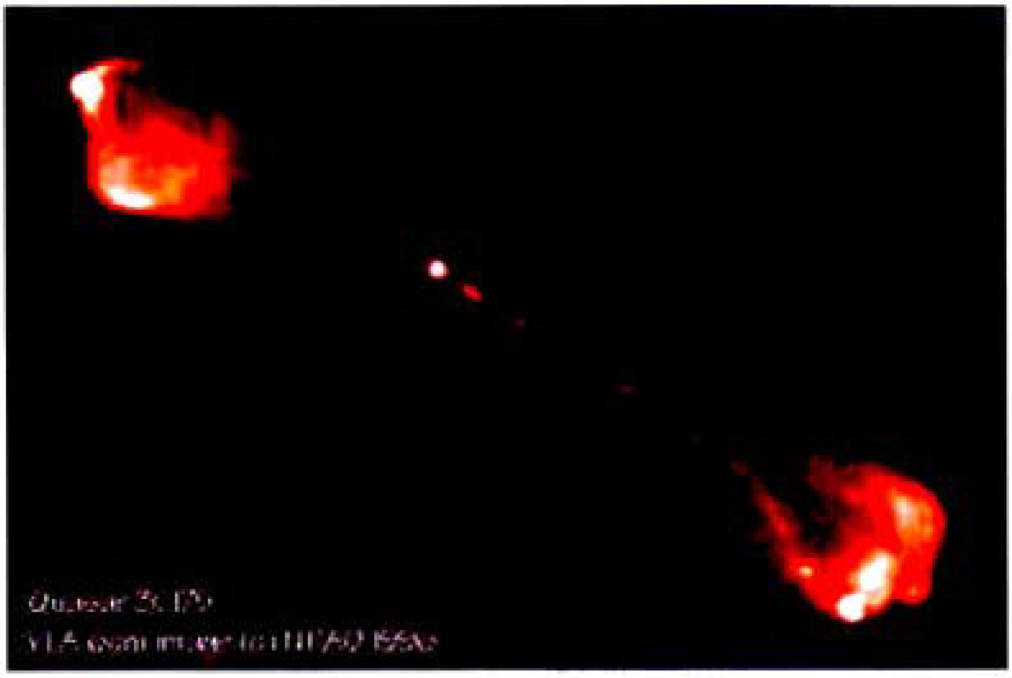

- Quasar at z=0.768
- Overall linear size 212/h kpc (Hubble constant H = 100h km/s/Mpc)
- Double lobes with prominent hot spots
- Narrow jet, no counterjet (Doppler hidden?)
- Jet brightens and bends as it enters its lobe
- VLA 4.9 GHz image at 0.35 arcsec resolution

See also Deep VLA Imaging of Twelve Extended 3CR Quasars, by Alan H. Bridle, David H. Hough, Colin J. Lonsdale, Jack O. Burns and Robert A. Laing, *The Astronomical Journal*, **108**, 766-820 (1994). Also related abstract from AAS Meeting #183.

Go back to:

3C263 = B1137+660

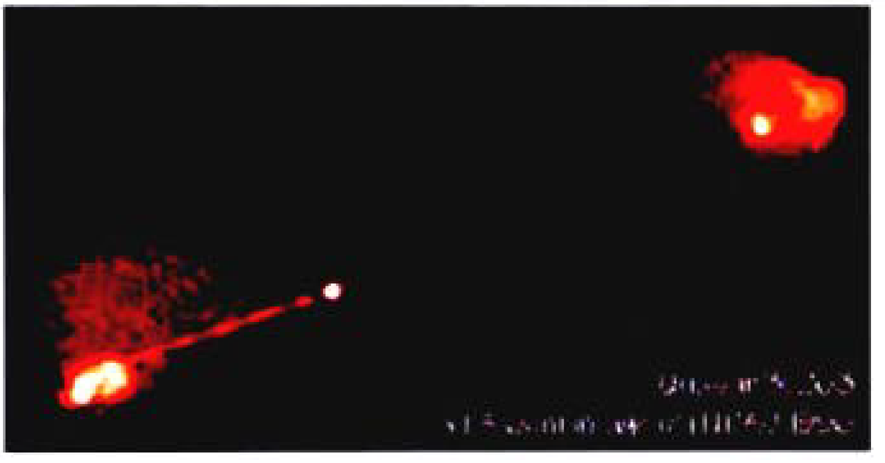

- FR II quasar at z=0.646
- Overall linear size 198/*h* kpc (Hubble constant H = 100*h* km/s/Mpc)
- Prominent hot spot and straight jet in East lobe
- Unusually large lobe-length asymmetry
- Superluminal motion at (1.3/*h*)c has been detected in the nuclear radio source
- VLA 4.9 GHz image at 0.36 arcsec resolution

See also Deep VLA Imaging of Twelve Extended 3CR Quasars, by Alan H. Bridle, David H. Hough, Colin J. Lonsdale, Jack O. Burns and Robert A. Laing, *The Astronomical Journal*, **108**, 766-820 (1994).

Go back to:

- Alan Bridle's Image Gallery
- Alan Bridle's Home Page
- NRAO Charlottesville Home Page
- NRAO VLA Home Page
- AstroWeb Home Page

HTML 3.2 last updated: **06 November 1996, 17:25 EST**

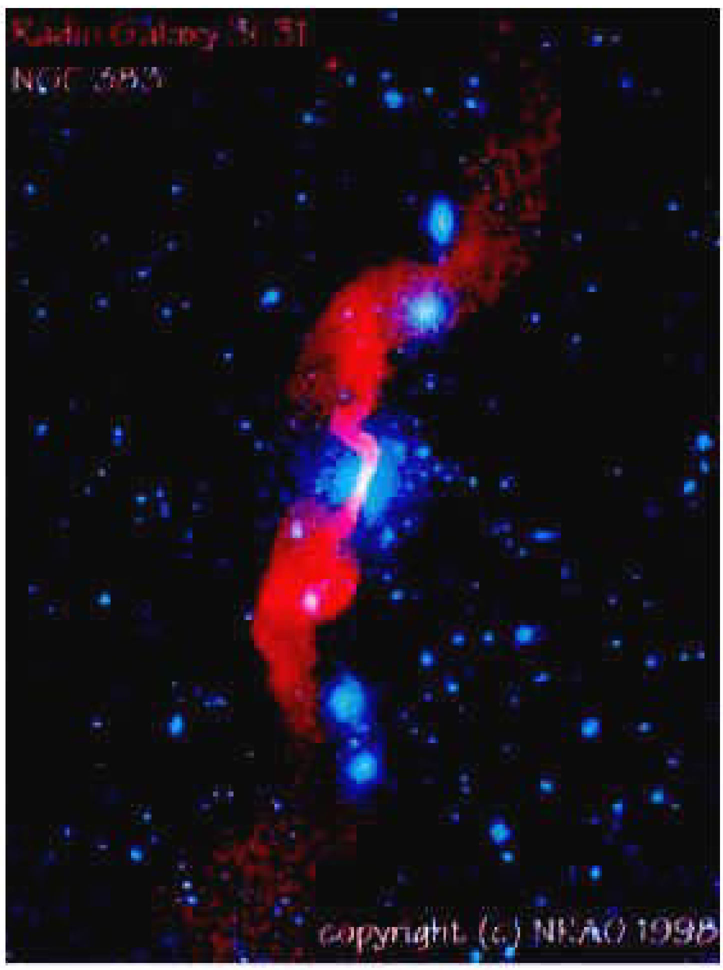
Radio Galaxy 3C 31
NGC 383
copyright (c) NRAO 1998

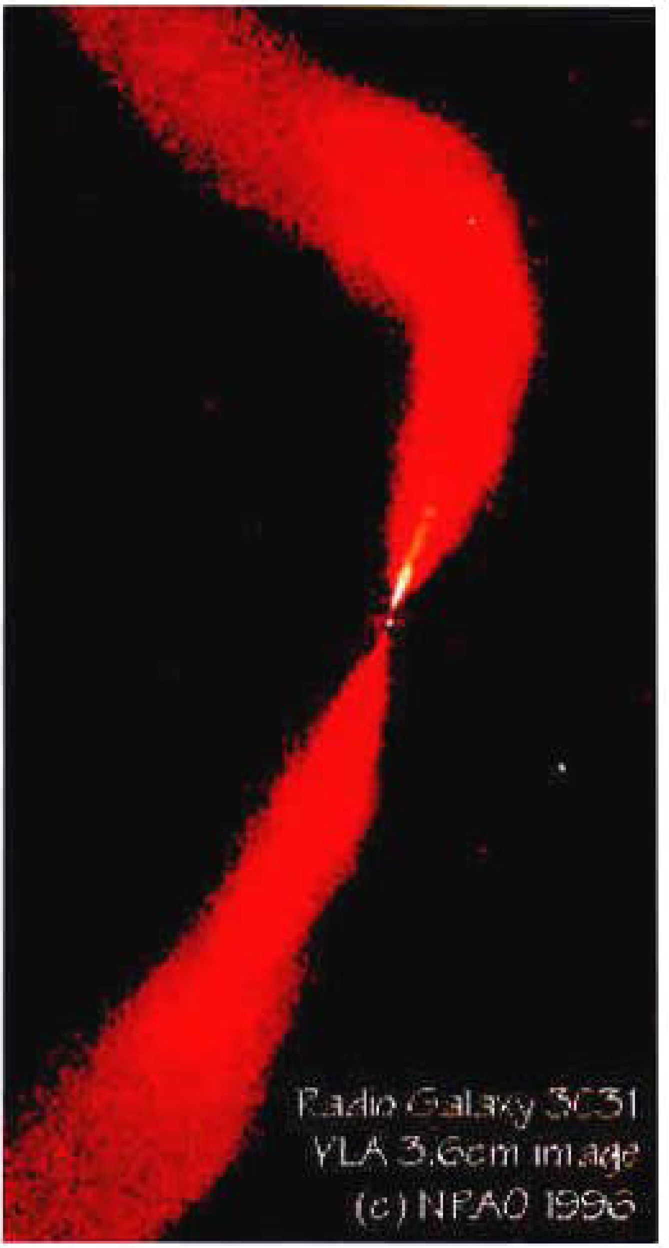
Radio Galaxy 3C31
VLA 3.6cm image
(c) NRAO 1996

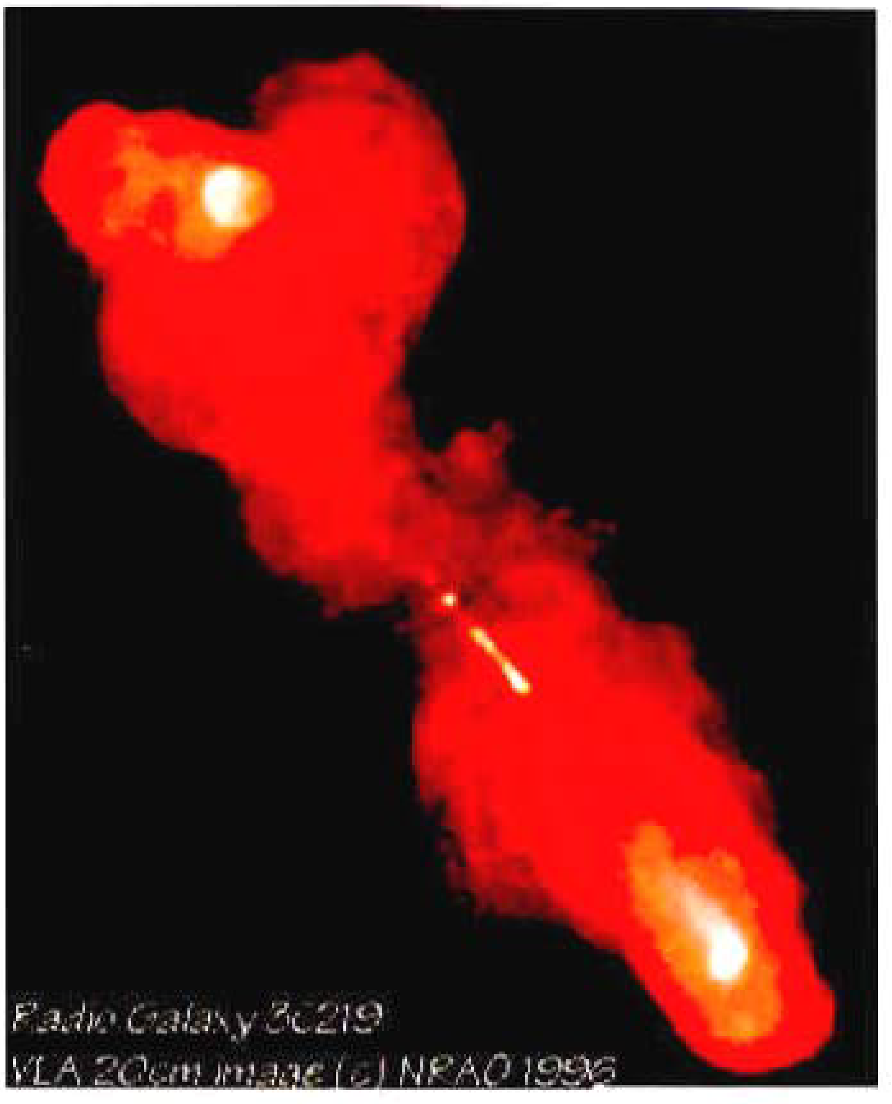
Radio Galaxy 3C219
VLA 20cm image (c) NRAO 1996

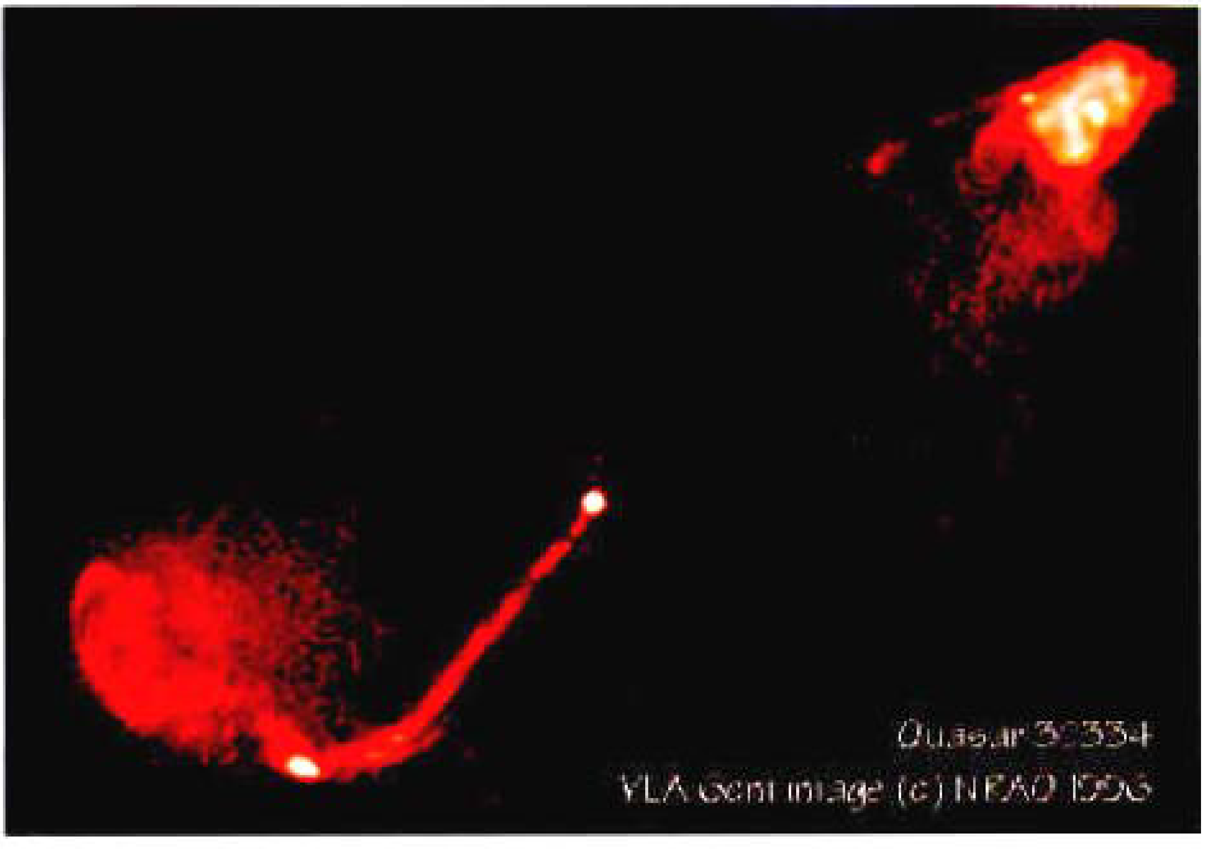
Quasar 3C334
VLA 6cm image (c) NRAO

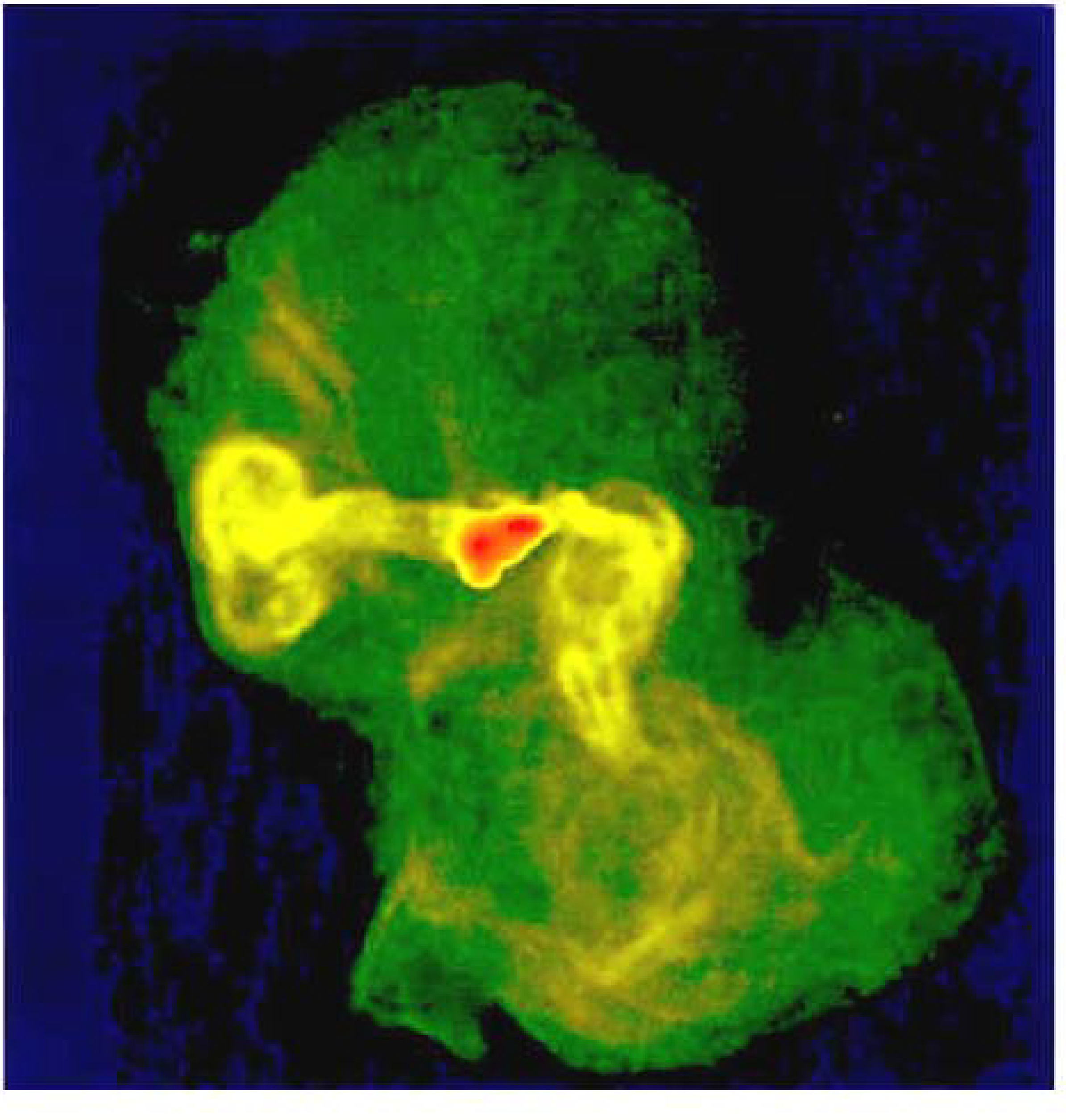

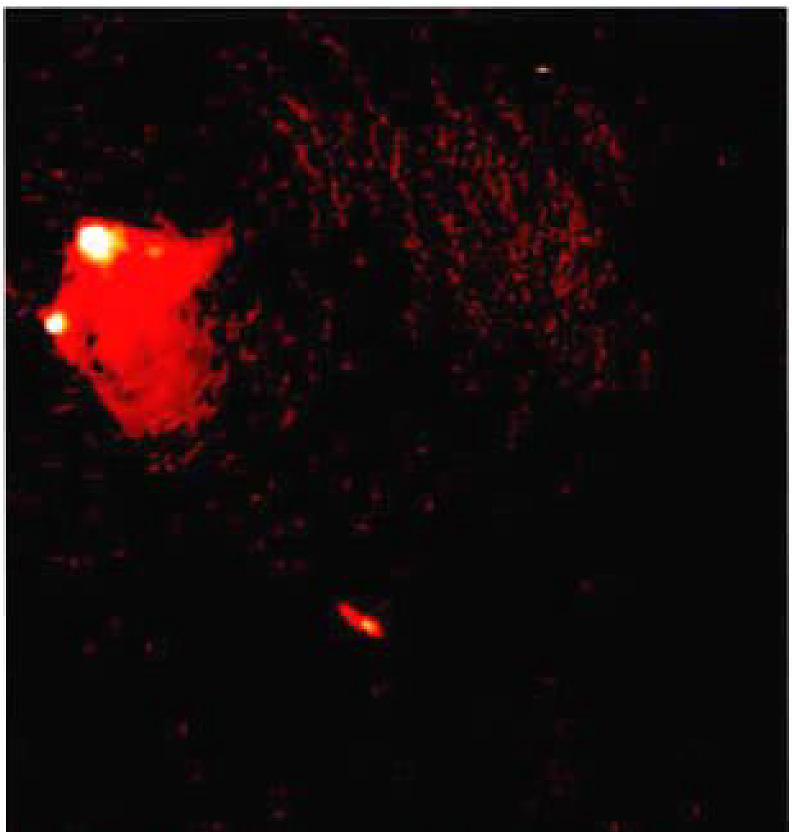
Quasar 3C351

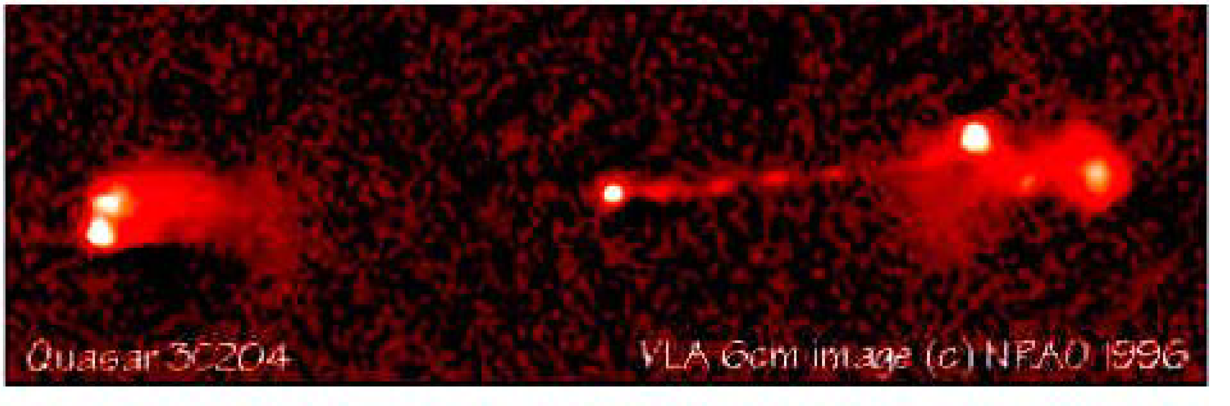
Quasar 3C204
VLA 6cm image (c) NRAO 1996

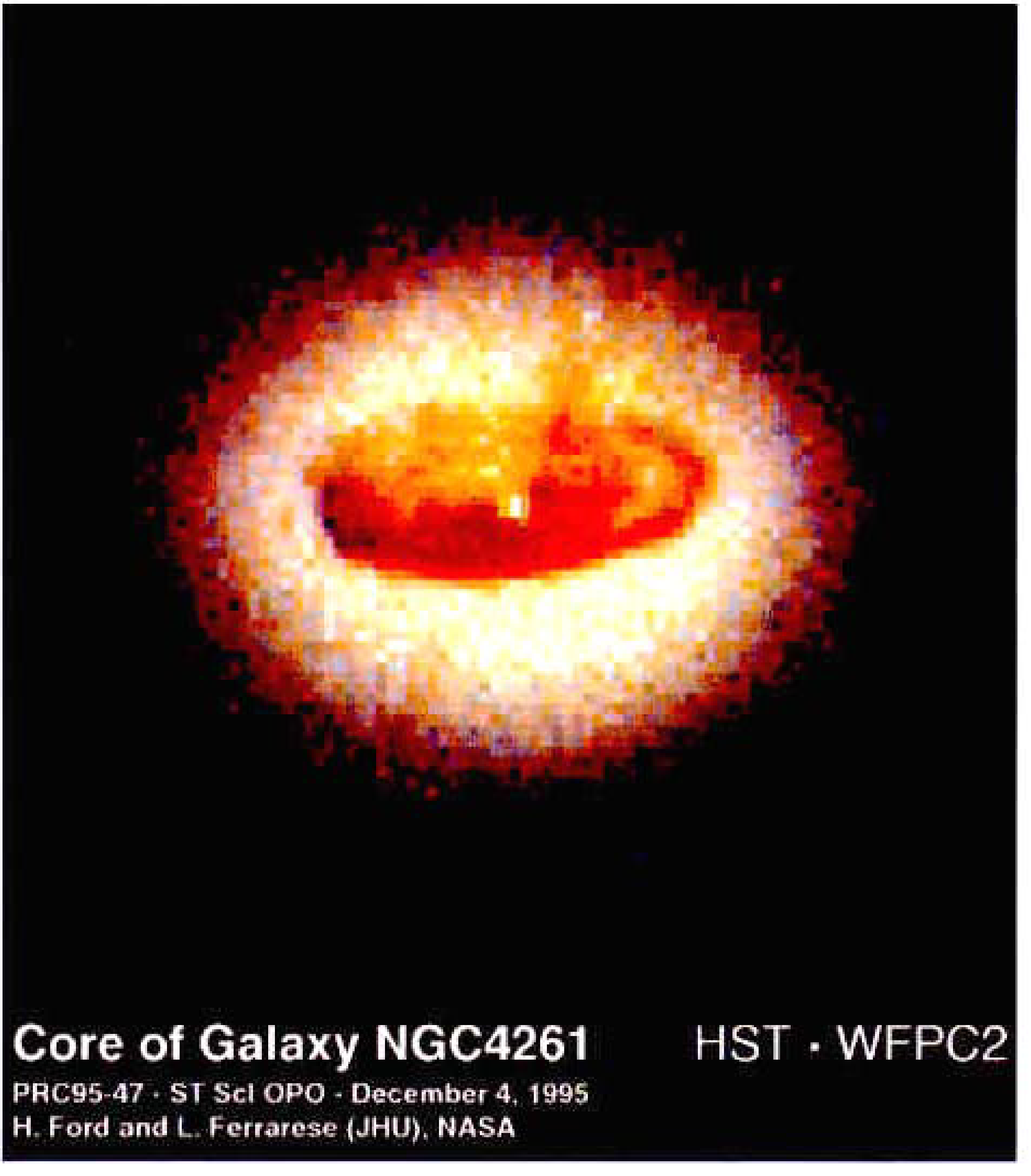
Core of Galaxy NGC4261
HST · WFPC2
PRC95-47 · ST ScI OPO · December 4, 1995
H. Ford and L. Ferrarese (JHU), NASA

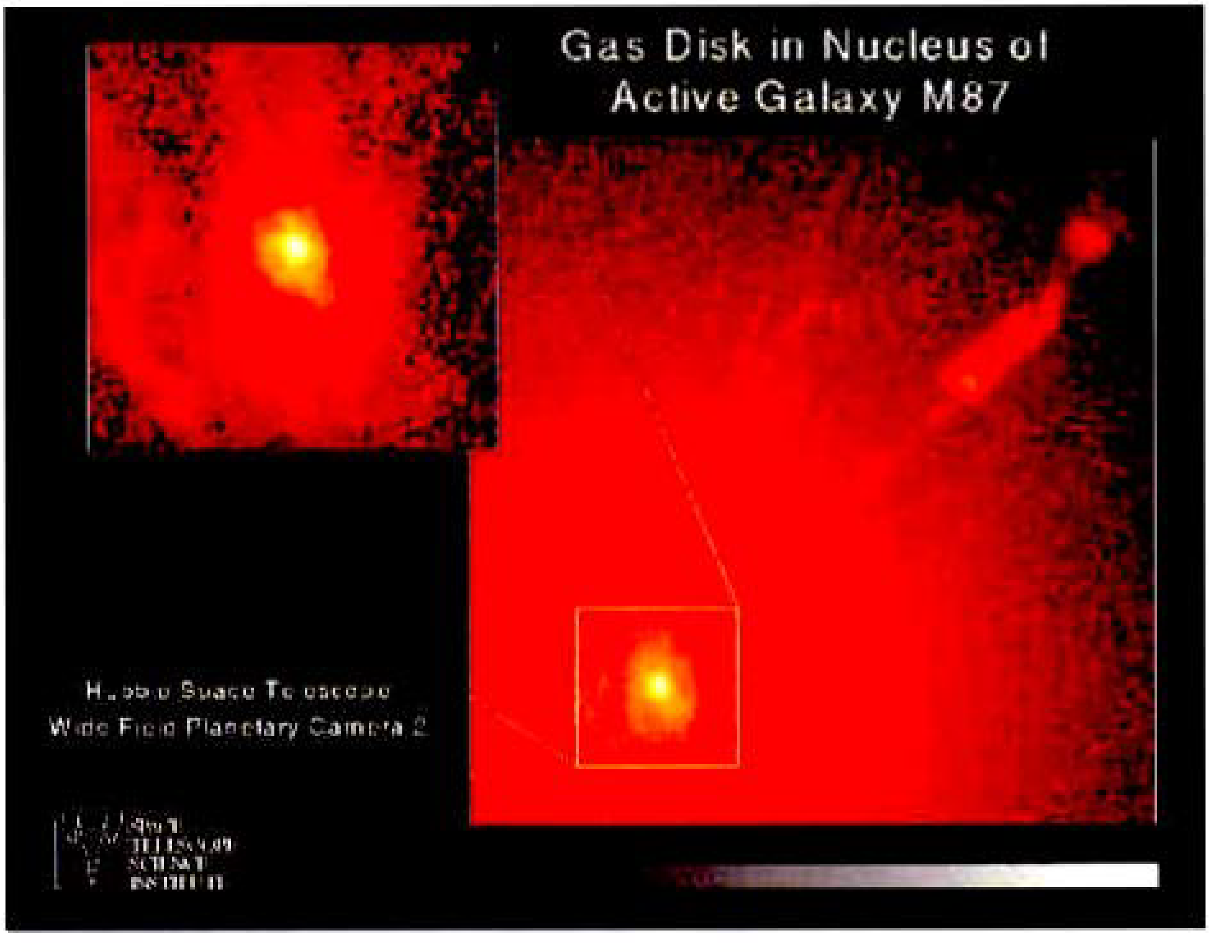
Gas Disk in Nucleus of
Active Galaxy M87
Hubble Space Telescope
Wide Field Planetary Camera 2

‘PLASMOIDS’

SOURCES OF COSMIC RAYS
VERY HIGH EN.
VERY LONG DIST.

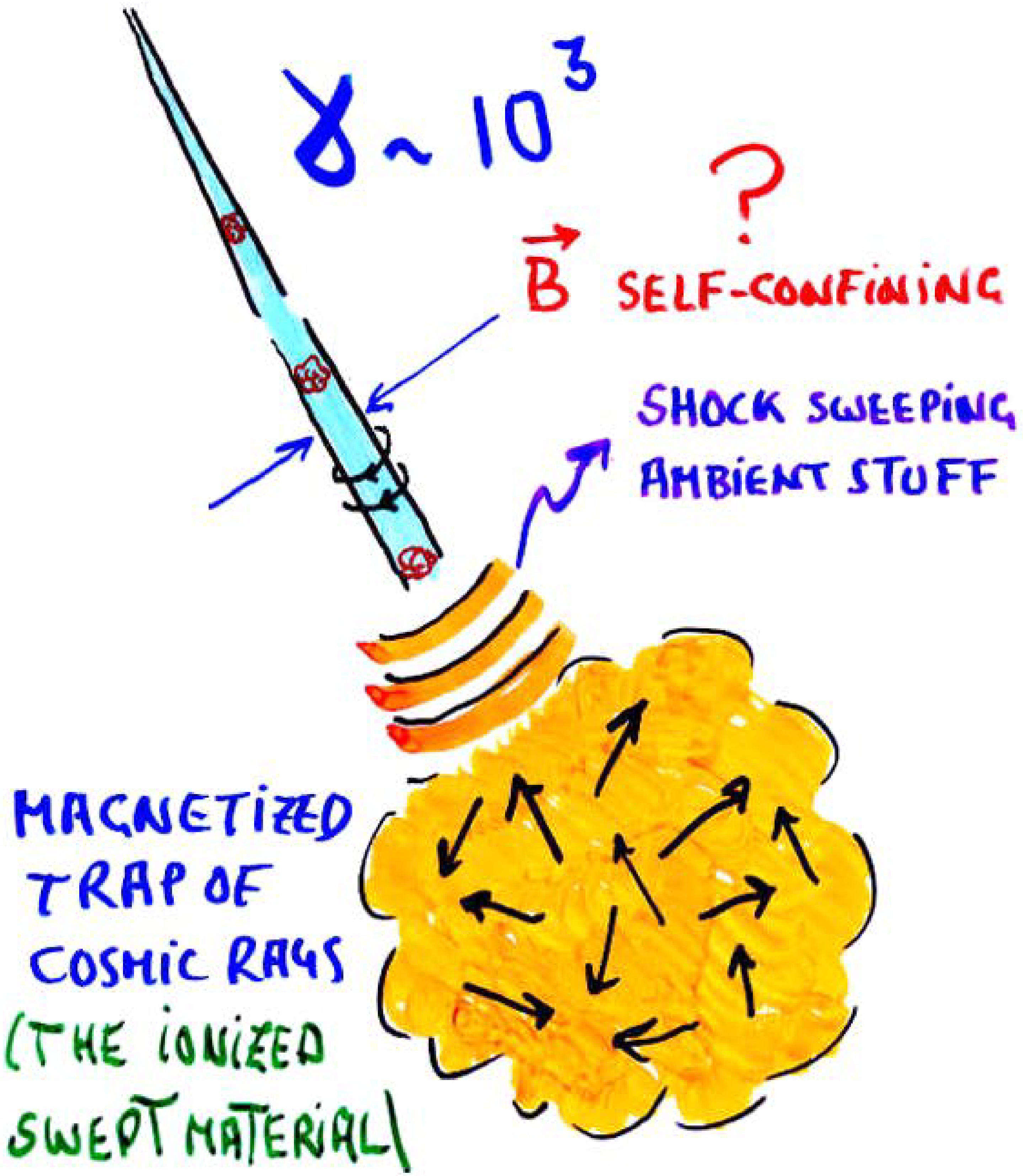

MIRABEL and Colls.

GRS 1915+105 ($l = 45°$, $b = 0°$)

ANTI-PARALLEL EJECTION OF A TWIN PAIR OF CLOUDS MOVING AT $V = 0.92c$ AND $\theta = 70°$

VLA-A λ 3.5 cm POSITION ACCURACY 0.02"

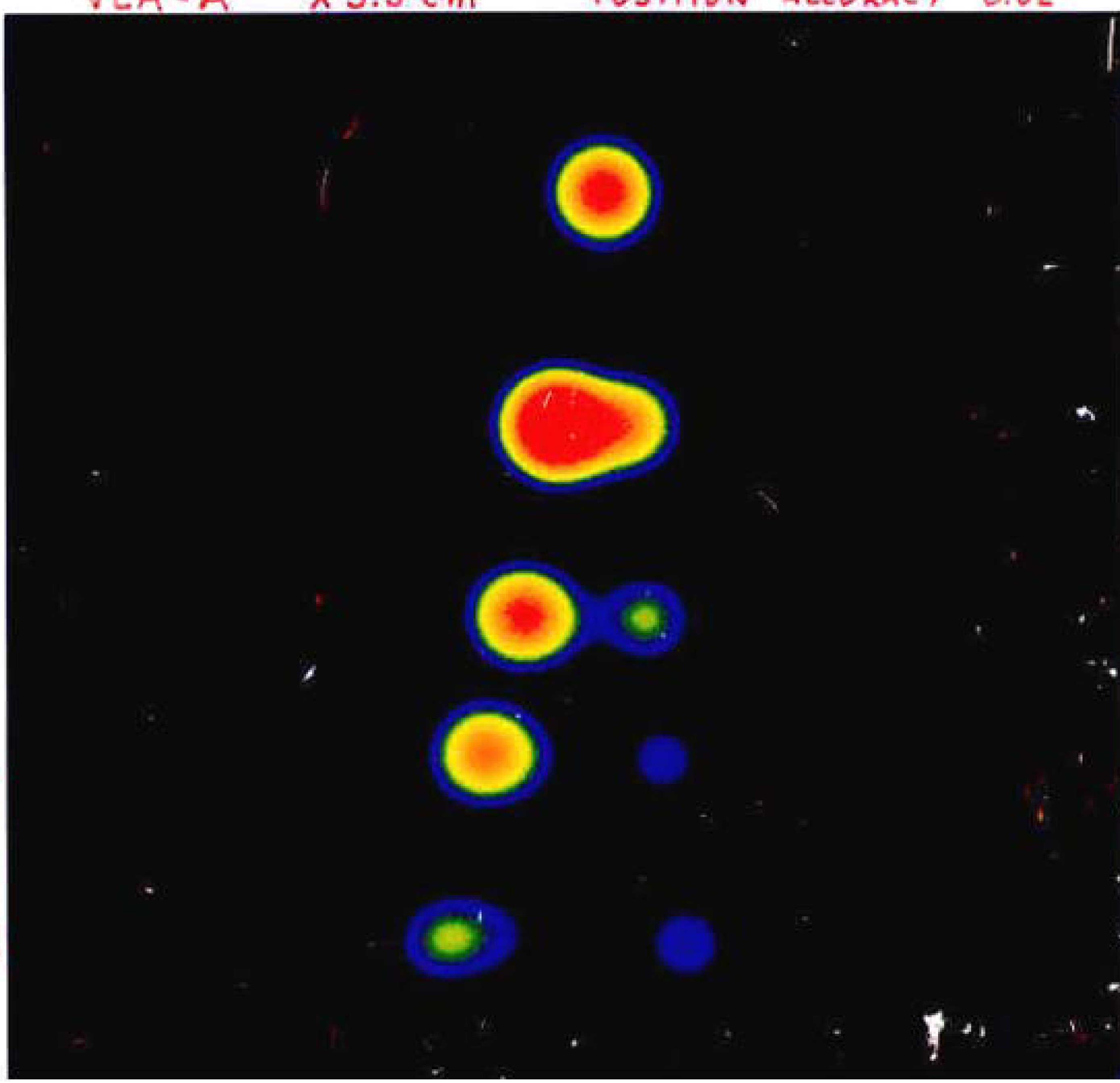

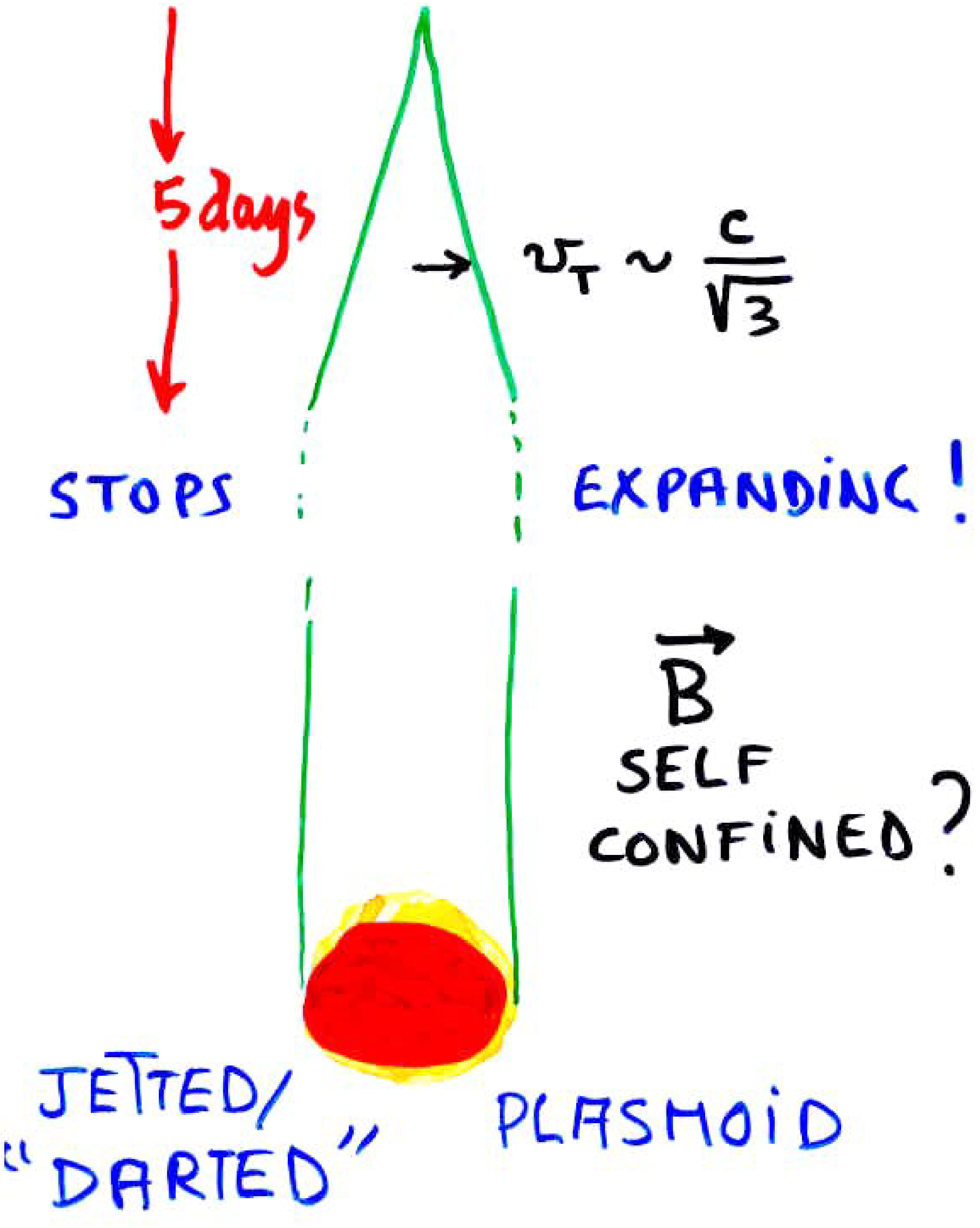
5 days
$v_T \sim \frac{c}{\sqrt{3}}$
STOPS
EXPANDING !
$\vec{B}$
SELF
CONFINED ?
JETTED/
"DARTED"
PLASMOID


JETS
GRBs

PROPERTIES OF GRBs
(γ RAY BURTS)

- **DISCOVERY** : VELA SATEL. 1960's
- **FRECUENCY** ~ 3/DAY
- **DURATION** $10^{-3}s \rightarrow 10^{3}s$

  SOMEWHAT BIMODAL

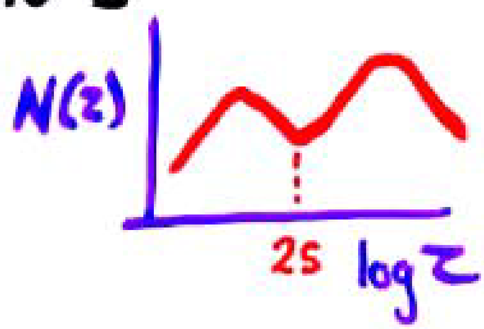

- **STRUCTURE**

  VERY VARIABLE, SUCCESIVE SHORT PULSES

- **VARIABILITY** : DOWN TO $10^{-3}s$

$c\tau = 300\,km$ VERY COMPACT SOURCE

SPECTRUM

$$\frac{dn_\gamma}{dE_\gamma} \propto E_\gamma^{-\alpha}$$

$\alpha \simeq 1.3 \rightarrow \alpha \simeq 2.3$

$\neq$ THERMAL

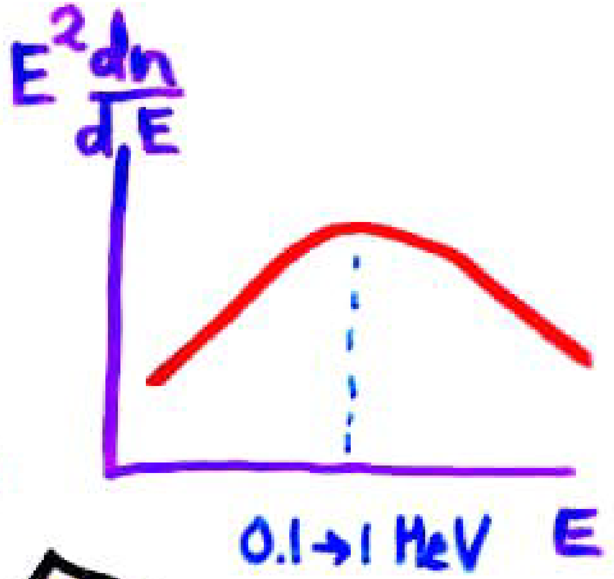

VERY LITTLE FLUX IN keV, GeV γs

DIRECTIONAL DISTRIBUTION

ISOTROPIC ← GALACTIC HALO

ISOTROPIC ← "COSMOLOGICAL"

AFTERGLOW

Radio → X ray

$\tau_{AG} \sim$ DAYS

BEPPO-SAX

ROSSI X-RAY TIMING-EXPLORER

⇒ PROMPT DIRECTIONAL LOCALIZ.

Gamma ray bursts of known redshift

GRB	z	Ref.	Fluence[a]	m(host)	Ref.
970228	0.695	1	1.1	$R = 25.3$	11
970508	0.835	2	0.3	$R = 25.1$	12
971214	3.418	3	1.1	$R = 26.2$	13
980425	0.0083	4	0.4	$R = 14.3$	14
980613	1.0964	5	0.2	$R = 24.1$	15
980703	0.966	6	4.6	$R = 22.6$	16
990123	1.600	7,8	51	$R = 23.7$	17
990510	1.619	9	2.6	$V > 28$	18
990712	0.430	10	—	$R = 21.7$	19

Table 1: a: BATSE γ-ray fluences in units of 10^{-5} erg cm^{-2}.
References: 1: Djorgovski et al. 1999b; 2: Metzger et al. 1997; 3: Kulkarni et al. 1998b; 4: Tinney et al. 1998; 5: Djorgovski et al. 1999a; 6: Djorgovski et al. 1998a; 7: Kelson et al. 1999; 8: Hjorth et al. 1999a; 9: Vreeswijk et al. 1999; 10: Galama et al. 1999; 11: Fruchter et al. 1999b; 12: Bloom et al. 1998a; 13: Odewann et al. 1998; 14: Kulkarni et al. 1998b; 15: Djorgovski et al. 1998c; 16: Bloom et al. 1999b; 17: Fruchter et al. 1999c; 18: Fruchter et al. 1999d. 19: Hjorth et al. 1999b

GRBs are
"COSMOLOGICAL"

GRB 990712 R-BAND AFTERGLOWS

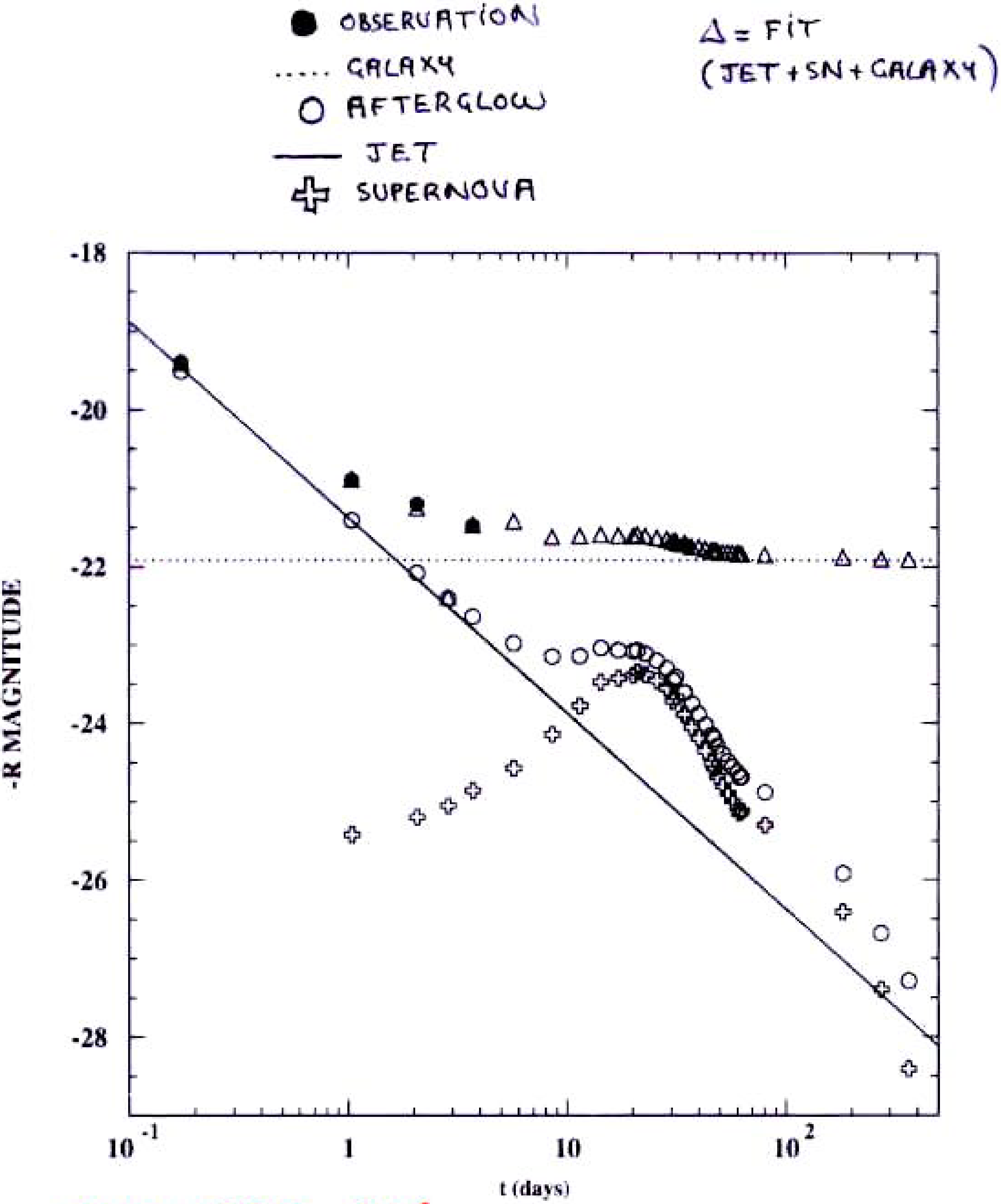

THE GRB-SN ASSOCIATION

Courtesy of ARNON DAR

○ = JET (—) + SN (✚)

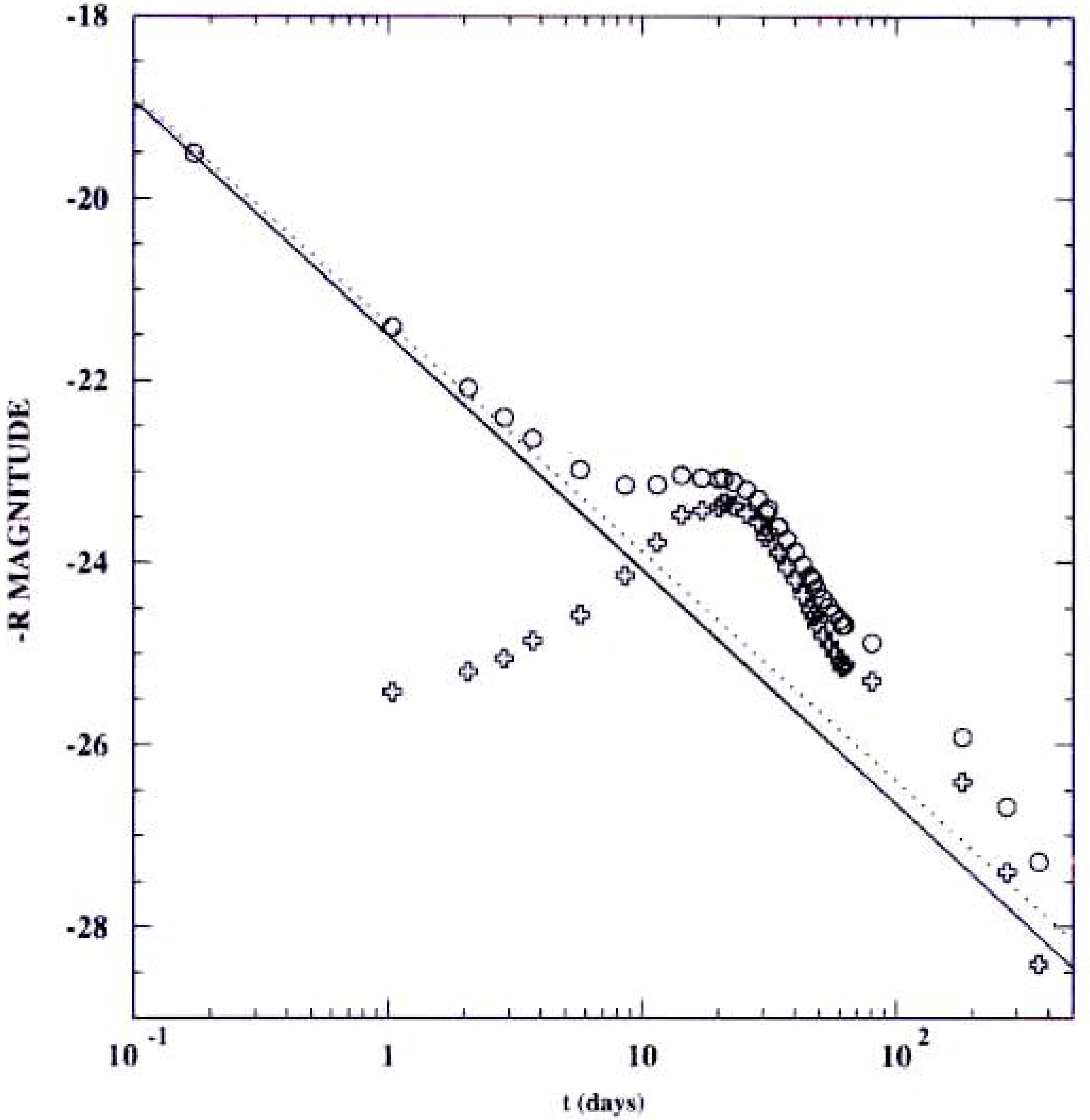

Courtesy of ARNON DAR

THE COSMOLOGICAL-GRB ENERGY CRISIS

- TYPICAL FLUENCE $F_\gamma \simeq 10^{-5}\,erg/cm^2$
- 'LUMINOSITY' DISTANCE

$$D_L(z\sim 1.2) \sim 2.5\,10^{28}\,cm$$

$$(\Lambda = 0,\ \Omega_M = 0.2,\ H_0 = 65\,km/s/Mpc)$$

$$E_\gamma = 4\pi\,\frac{D_L^2 F_\gamma}{1+z} \sim 3.7\,10^{52}\,erg$$

$$E_\gamma(\text{GRB990123}) \sim 3.4\,10^{54}\,erg$$

★-ENERGIES

$$\frac{G M_\odot^2}{r_{NS}} \sim 10^{53}\,erg \qquad M_\odot c^2 \sim 1.8\,10^{54}\,erg$$

$$\eta(\Rightarrow \gamma\ \text{RAYS}) \sim 10^{-4}$$

STRONG INDICATION AGAINST SPHERICITY

INDICATIONS of RELATIVISTIC MOTION

FAST VARIABILITY (SMALL SIZE)

LARGE LUMINOSITY

OPTICALLY THICK TO $\gamma\gamma \rightarrow e^+e^-$

EXPECT CUTOFF $F(E_\gamma > 0.5\text{-}1\,\text{MeV})$

NOT SEEN !

BOO OOOST !!

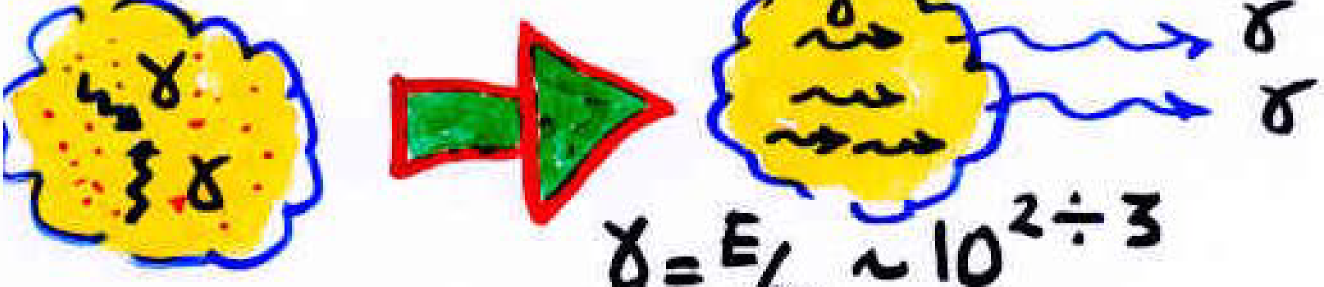

$\gamma = E/m \sim 10^{2 \div 3}$

e^+e^- CUTOFF RISES TO UNOBSERV. HIGH ENERGY (FLUX SMALL)

Sadly and Incidentally

MECHANISM THAT MAKES THE γ'S OF GRBs IS NOT DETERMINED

<u>POSSIBILITIES</u> (examples)

-  MERGER OF PLASMOIDS
- $e^+ e^- \longrightarrow 2\gamma_{GRB}$
- $(A,Z)^{++\cdots} + \gamma_{\star} \rightarrow$ EXCITED $\rightarrow \gamma_{GRB}$
- $\overrightarrow{e} + \gamma_{\star} \rightarrow e' + \gamma_{GRB}$

~isotropic in PLASMOID'S FRAME

NON ISOTROPIC

- $P_{PLASMOID} + P_{ISM} \rightarrow \pi^0 \rightarrow 2\,\gamma_{GRB}$

WHAT IS MOVING FAST AND IS NOT SPHERICAL

¿?

A JET!

$\Rightarrow \gamma \equiv \Gamma$!

$$F(\nu_P) \propto \nu_P^{-\alpha} \quad \text{ISOTROPIC}\Big|_P$$

$$F(\nu) \propto \left(\frac{2\Gamma}{1+\Gamma^2\theta^2}\right)^3 F\left(\nu\,\frac{1+\Gamma^2\theta^2}{2\Gamma}\right)$$

$$= \frac{1}{\nu^\alpha}\left(\frac{2\Gamma}{1+\Gamma^2\theta^2}\right)^{3+\alpha}$$

BEAMED RADIATION

$$\theta \sim \frac{1}{\Gamma} \qquad \Delta\Omega \sim \frac{\pi}{\Gamma^2}$$

- SOLVES THE ENERGY CRISIS
- CHANGES "REAL" GRB RATE

SOLUTION TO ENERGY CRISIS

$$\Delta\Omega \sim \pi\, 10^{-6} \left(\frac{10^3}{\Gamma}\right)^2$$

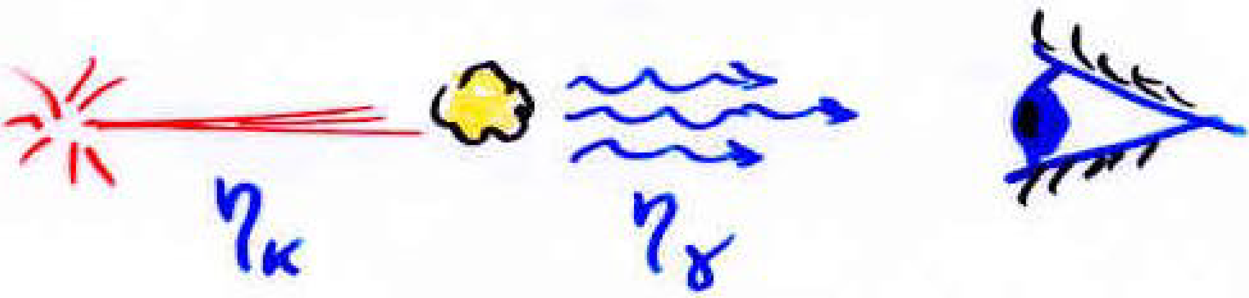

TOTAL ENERGY DEDUCED FROM FLUENCE IS REDUCED BY $\Delta\Omega/4\pi$

$\eta_K \sim 1\%$ $\eta_\gamma \sim 1\%$

$\eta_{TOT} \sim 10^{-4}$ STILL ACCEPTABLE FOR ★-FUELED ENGINE

NS KICKS & JETS (DAR & PLAGA)

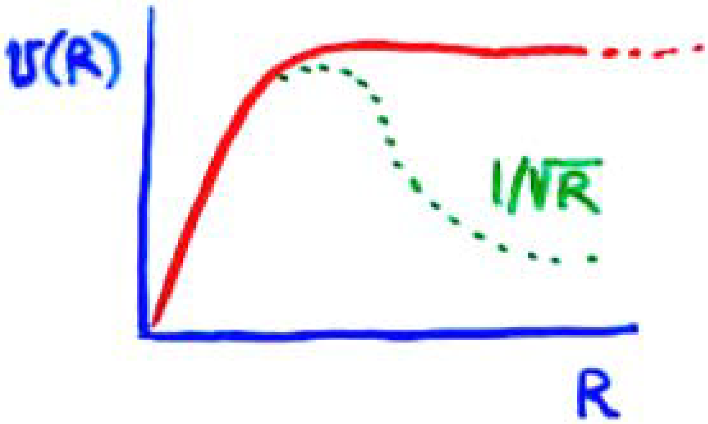

$v_\star \sim v_\odot \sim 250\ \mathrm{km/s}$

$v_{NS} \sim 450 \pm 90\ \mathrm{km/s}$

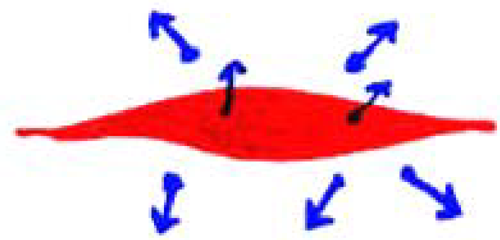

$E_p \sim v M_{NS} c \sim 4\, 10^{51}\,\mathrm{erg}$

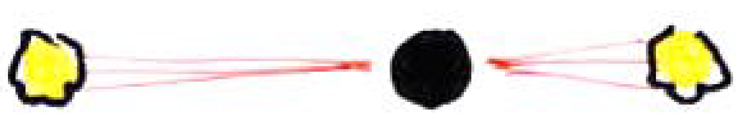

$E_p \sim 10^{52}\,\mathrm{erg}$?

$* \ \eta \sim 10^{-4} \Rightarrow$ GRB OK

HYPOTHESIS GIVES O(MAGNITUDE) OF KINETIC ENERGY OF THE JETTED (DARTED) PLASMOID

GRBs AND COSMIC RAYS ?

PLASMOID DECELERATION IN GALAXY

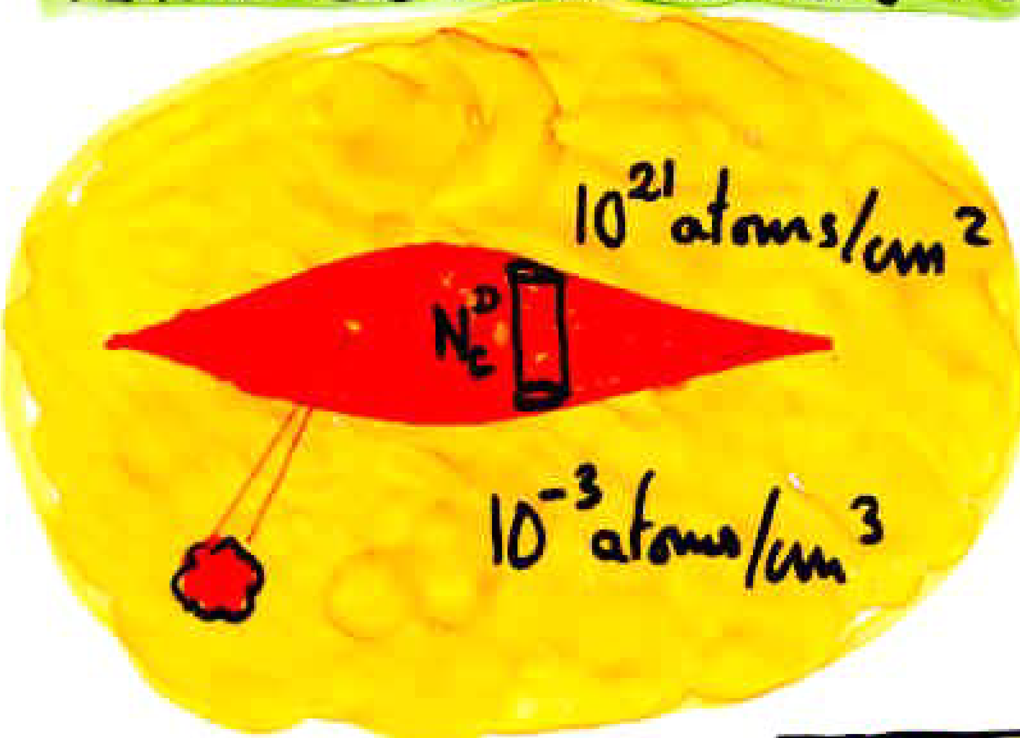

PLASMOID SWEEPS

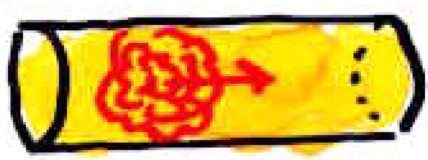

$O(0.01pc)$

$E_p \simeq 10^{52}$ ergs $\quad m\Gamma \rightarrow 2m\frac{\Gamma}{2}$

$$E_p = \rho \, \pi R_p^2 \, \ell$$

$$N_c = \frac{\rho \ell}{m_p} \sim 2\,10^{21}/cm^2$$

$$N_c \gtrsim N_c(\text{DISK})$$

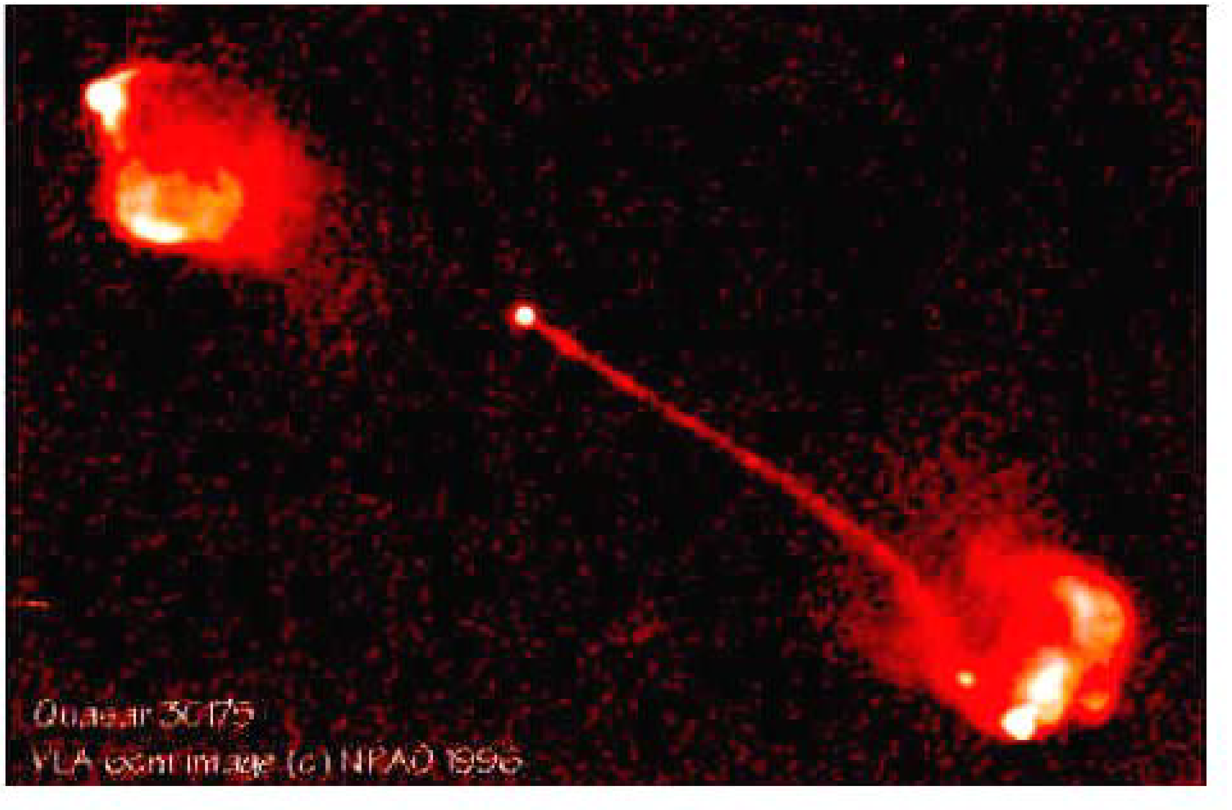
Quasar 3C175
VLA 6cm image (c) NRAO 1996

DAR - PLAGA

CR $\in$ DISK + HALO

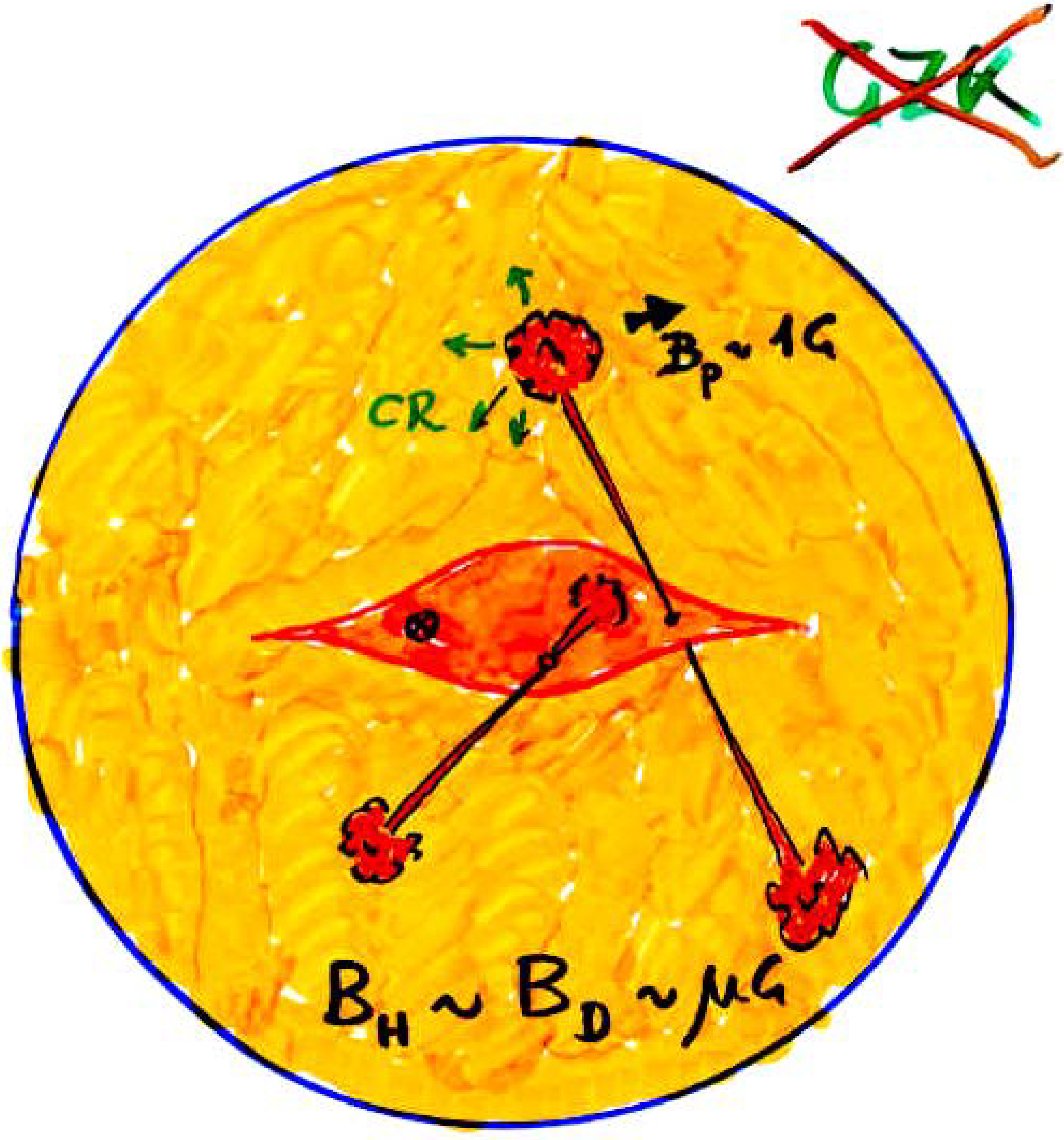

ALSO, IF POINTING FROM A DISTANT GALAXY : γ-RAY BURSTS

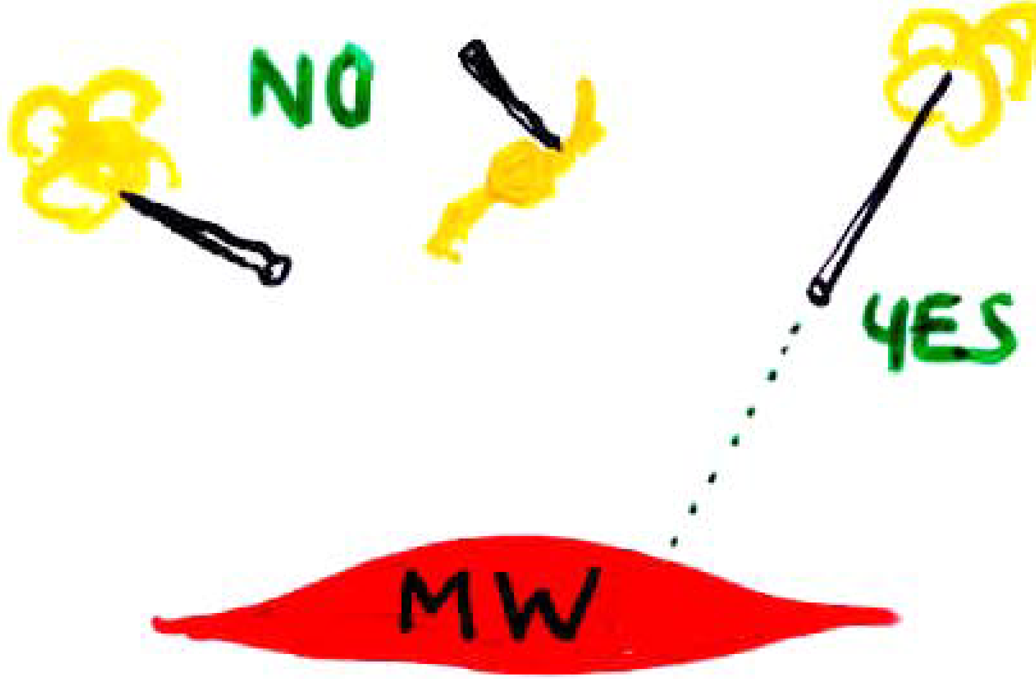

G.R.B.

DAR et al
VIETRI
WAXMAN
MILGROM/USOV

PERHAPS GAMMA RAY BURSTS [E-GALAC]

ARE VERY VERY JETTY

$\frac{\Delta\Omega}{4\pi}$ PROBABILITY OF POINTING TO YOU

RELATIVISTIC SHOCKS IN COLLISIONLESS PLASMAS

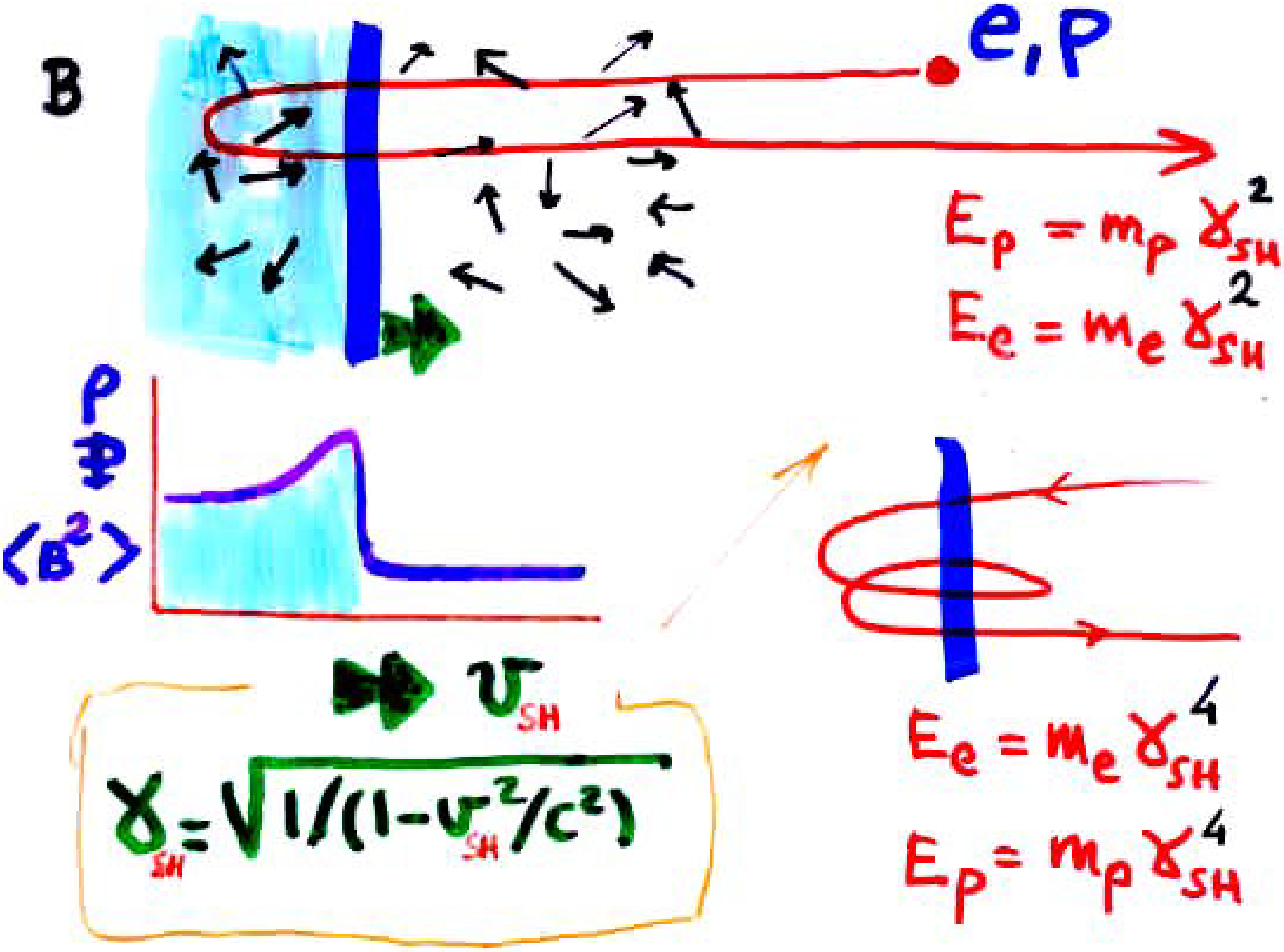

DEATH OF A PING-PONG BALL

JAR GORBANOV

DAR, DAR-PLACA

$$\frac{dN_{OBS}}{dE} \propto \frac{dN_{SOURCE}}{dE}\, \tau^{GALAXY}_{ACCUM}(E)$$

$$\downarrow E^{-\sim 0.6}$$

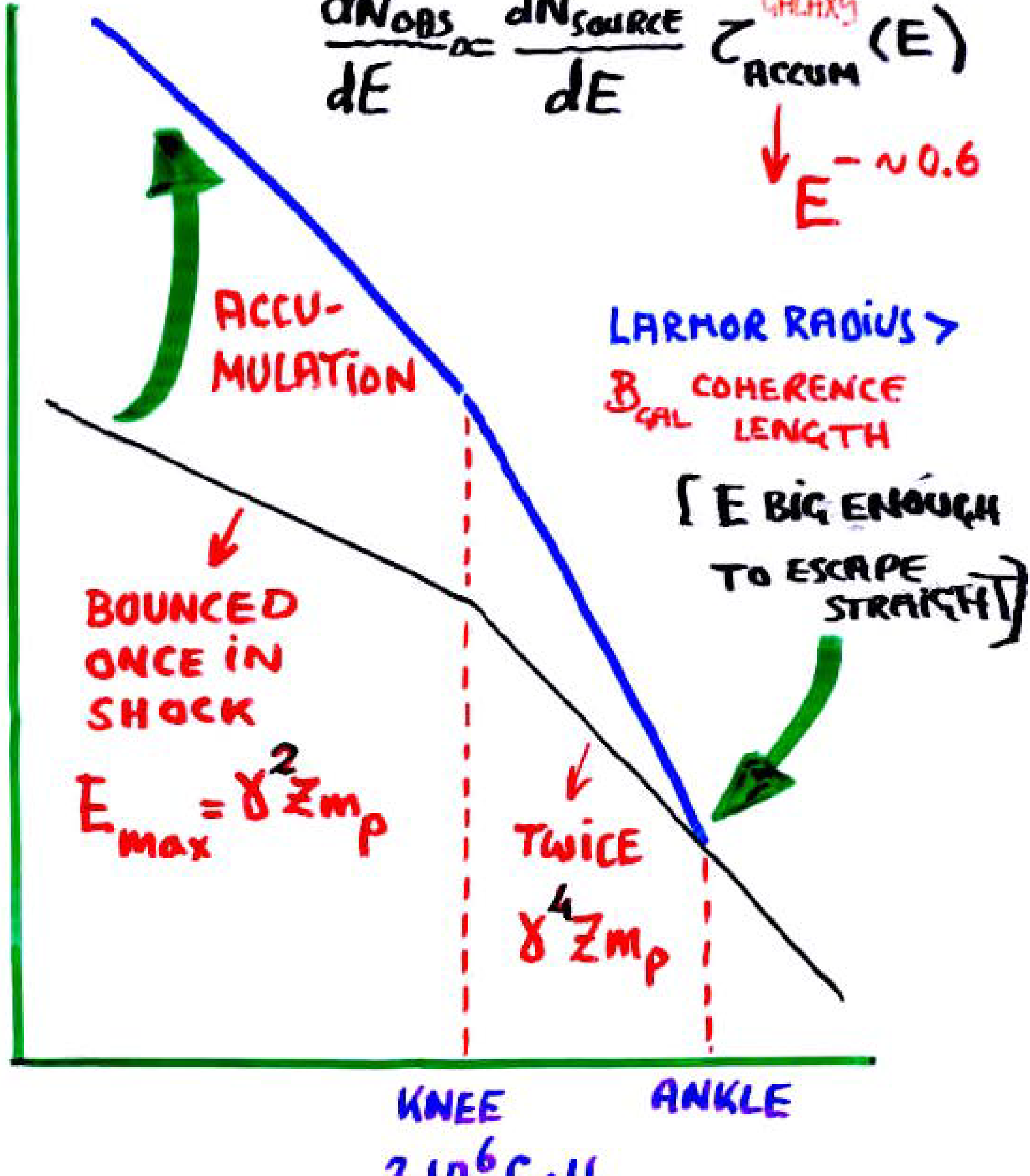

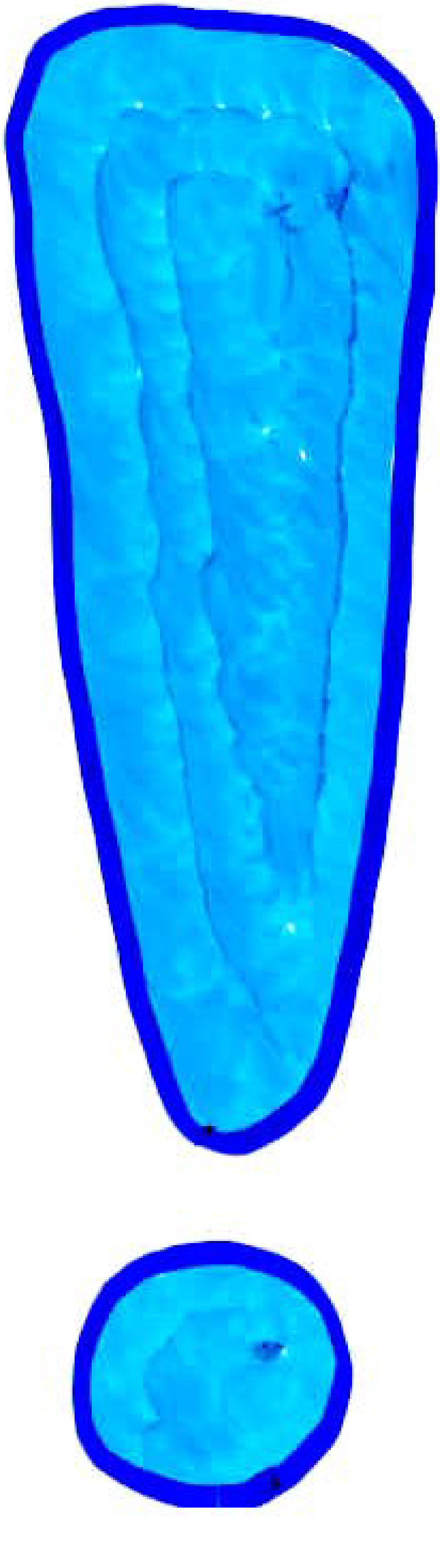

NOT

discuss the origin of

GAMMA RAY BURSTS

BUT

THE LOCATION OF

"RESIDENCE" OF

COSMIC RAYS

1rst TALK

COSMIC RAY (CR) CONUNDRA

ORIGIN OF CRs ?

VERY HIGH ENERGY CRs?

JETS IN ASTROPH.

GAMMA RAY BURSTS

TOTAL E-OUTPUT

ABSENCE OF $\gamma\gamma \to e^+e^-$ CUTOFF

$\Big\}$ γRBs are JETTY

Astr. and Astrophys. 1998

THE RADIO HALO OF THE EDGE-ON GALAXY

NGC 5775

$\theta_i \approx 84^\circ$

$d \approx 28.6$ Mpc

$$\frac{dN_e}{dE} \propto E^{-\beta}$$

$\beta_{disk} \sim 2.2$

$\beta_{halo} \sim 3.2$

$43 \times 22 \ (\mathrm{kpc})^2$

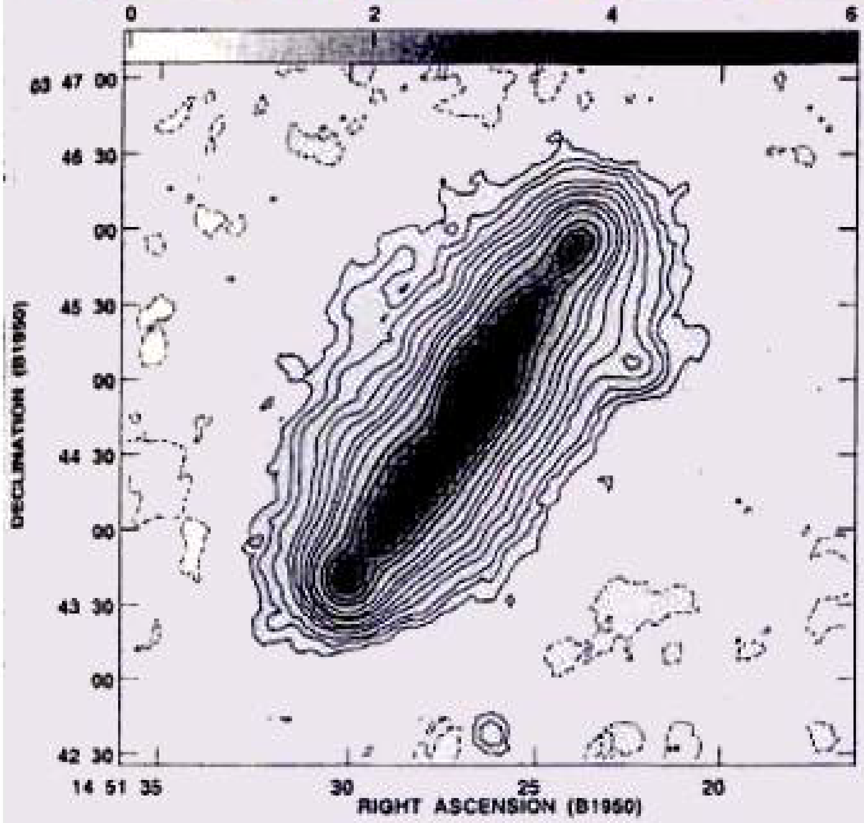

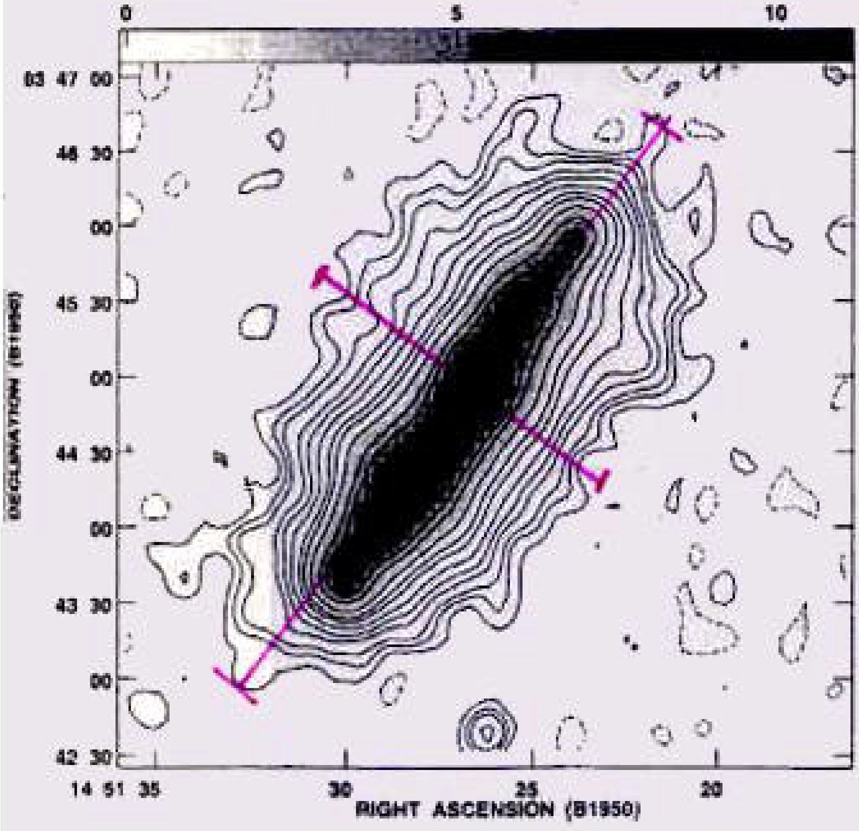

Fig. 2. a The 20 cm radio continuum image used in the analysis. With a restoring beam of 15″ × 13″, it represents the net result of combining the B, C and D array data. The *rms* noise in this map is 25 μJy/beam. The contours represent 1, 2, 3, 5, 7, 10, 15, 20, 30, 50, 70, 100, 125, 150, 175, 200, 300, 500, 750 and 1000 times 70 μJy/beam. **b** The 6 cm continuum image used in the analysis. With a restoring beam of 15″ × 13″, it represents net result of combining the C and D array data. The *rms* noise in this map is 25 μJy/beam. The contours represent 1, 2, 3, 5, 7, 10, 15, 20, 30, 50, 70, 100, 125, 150, 175 and 200 times 30 μJy/beam.

Duric et al. A&A

M82 STAR-BURST GALAXY

$\mathrm{RATE}(\star) \gtrsim 50\, R(\star)|_{\mathrm{NORMAL}}$

$\sim 1\,\mathrm{kpc}$